Life-history and deleterious mutation rate coevolution

Piret Avila* and Laurent Lehmann

Department of Ecology and Evolution, University of Lausanne

Biophore, 1015 Lausanne, Switzerland

*Corresponding author: piret.avila@gmail.com.

Abstract

The cost of germline maintenance and repair gives rise to a trade-off between lowering the deleterious mutation rate and investing into life-history functions. Life-history and the mutation rate therefore coevolve, but this joint evolutionary process is not well understood. Here, we develop a mathematical model to analyse the long-term evolution of traits affecting life-history and the deleterious mutation rate. First, we show that under certain biologically feasible conditions, the evolutionary stable life-history and mutation rate can be characterised using the basic reproductive number of the least-loaded class. This is the expected lifetime production of offspring without deleterious mutations born to individuals with no deleterious mutations. Second, we analyse two specific biological scenarios: (i) coevolution between reproductive effort and mutation rate and (ii) coevolution between age-at-maturity and mutation rate. These two scenarios suggest two broad results. First, the trade-off between lowering mutation rate vs investing into life-history functions depends strongly on environmental conditions and baseline mutation rate. Second, the trade-offs between different life-history functions can be strongly affected by mutation rate coevolution and higher baseline mutation rates select for faster life histories: (i) higher investment into fecundity at the expense of survival and (ii) earlier age of maturation at smaller sizes.

Keywords: life-history evolution, mutation accumulation, adaptive dynamics, cost of fidelity, mutation rate evolution

1 Introduction

Maintaining and accurately transmitting genetically encoded information is central for every living organism. Mutations induce errors in the processing of genetic information and their effects on fitness are generally (mildly) deleterious (Eyre-Walker and Keightley, 2007). Therefore, it is likely that selection primarily favours a reduction of the mutation rate of organisms (Sniegowski et al., 2000). Yet, investing resources into germline maintenance and repair is physiologically costly (Kirkwood, 1986; Maklakov and Immler, 2016; Monaghan and Metcalfe, 2019; Chen et al., 2020). Therefore, the balance between selection against deleterious mutations driving for lower mutation rates and selection for reduced physiological cost increasing mutation rates are expected to lead to an evolutionary equilibrium rate of mutation. This argument has been formalised in a number of classical population genetic models assuming semelparous reproduction to show that evolution indeed favours a positive evolutionary stable mutation rate (e.g. Kimura, 1967; Kondrashov, 1995; Dawson, 1998, 1999). These studies emphasise the role of physiological cost of germline fidelity in explaining the patterns of mutation rates, but do not connect the cost of germline fidelity explicitly to life-history evolution, which depends on underlying physiological trade-offs.

Indeed, a central premise made in life-history theory is that life-history trade-offs are mediated through allocation of resources to different life-history functions, such as growth, reproduction, repair and maintenance of soma, or information gathering and processing (Stearns, 1992; Roff, 2008). Since germline maintenance and repair takes a toll on available resources, mutation rate evolution and life-history evolution are tied together through a resource allocation trade-off. This implies that the rate of deleterious mutations co-evolves with life-history and affects various life-history traits, such as reproductive effort, age-at-maturity, adult body size, and expected lifespan. While the effect of unevolving (fixed) mutation rate on life-history trade-offs have been studied before (e.g. Charlesworth, 1990; Dańko et al., 2012), these models suggest that a relatively high level of mutation rates is needed for mutation accumulation to alter life-history trade-offs. This led to the conclusion that mutation accumulation is a minor force in shaping life-history traits (Dańko et al., 2012). But these studies view mutation rates as non-adaptive fixed traits acting only as a hindrance for adaptive life-history evolution. Hence, no study has yet investigated the joint adaptive coevolution of both deleterious mutation rates and general life-histories in age-structured populations.

The aim of this paper is to start to fill this gap by formally extending evolutionary invasion analysis–"ESS" theory–(e.g., Maynard Smith, 1982; Eshel and Feldman, 1984; Metz et al., 1992; Charlesworth, 1994), which has been routinely applied to life-history evolution (e.g., Michod, 1979; Stearns, 1992; Perrin, 1992; Charlesworth, 1994; Day and Taylor, 2000), to the case where life-history trait(s) evolving by selection also act as modifier(s) of deleterious mutations rates. This covers the situation where life-history resource allocation schedules evolve on a background where deleterious mutation accumulation can occur. Our formalisation thus aims at integrating both the standard theories of life-history evolution and deleterious mutation accumulation for direct selection on mutation rates.

The rest of this paper is organised into two parts. First, we characterise the invasion process of a mutant life-history trait affecting the load of deleterious mutations accumulation in an age-structured population. We show that ascertaining the joint evolutionary stability of life-history schedules and mutation rates of deleterious mutations is usually complicated, but under certain biologically feasible conditions; in particular, when the zero mutation class (least-loaded class) dominates the population in frequency, evolutionary stability can be ascertained from the basic reproductive number of the least-loaded class alone (expected lifetime production of offspring with no mutations born to individuals with no mutations). Second, we analyse and solve two concrete biological scenarios: (i) coevolution between reproductive effort and mutation rate, where individuals face a trade-off between allocating resources to survival, reproduction and germline maintenance and repair and (ii) coevolution between age-at-maturity and mutation rate, where individuals face a trade-off between allocating resources to growth, reproduction and germline maintenance and repair. These scenarios allow us to illustrate the applicability and usefulness of the basic reproductive number of the least-loaded class to ascertain evolutionary stable life-history schedules and mutation rates, demonstrate how results from our analysis match with individual-based simulations, and reveal some findings about how life-history co-evolves with mutation rates.

2 Model

2.1 Main biological assumptions

We consider an asexually reproducing panmictic population of large but bounded size through density-dependent regulation. This population is structured into age classes with each individual undergoing development, birth, and death. An individual at age a is characterised by an evolving trait $\theta(a)$ and we consider both discrete and continuous time age classes. As such, a is an element of a set $\mathcal{T}$ of age classes that is either a set of non-negative integers or a set of non-negative real numbers (i.e., respectively $a \in \mathbb{N}$ or $a \in \mathbb{R}_+$). The key feature of trait $\theta(a) = (\boldsymbol{u}(a), n_{\mathrm{m}}(a))$ is that it consists of two components. The first component, $\boldsymbol{u}(a)$, is the individual's life-history trait or control variable; namely, a resource allocation decision at age a to different classic life-history functions (i.e. growth, reproduction, or somatic maintenance, see e.g. Stearns, 1992; Perrin, 1992; Perrin and Sibly, 1993; Day and Taylor, 2000). We denote by $\boldsymbol{u} = \{\boldsymbol{u}(a)\}_{a\in\mathcal{T}}$ the real-valued function describing the whole life-history schedule or path. This consists of the (finite or infinite) collections of all pointwise, possibly multidimensional, values $\boldsymbol{u}(a)$ of the trait on the space $\mathcal{T}$ (formally, $\boldsymbol{u}$ is assumed to belong to the compact set $\mathcal{U}[\mathcal{T}]$ of pointwise continuous feasible controls of range $\mathcal{U}$ and domain $\mathcal{T}$). The second component, $n_{\mathrm{m}}(a)$, represents the number of deleterious germline mutations an individual at age a carries. Hence, $n_{\mathrm{m}}(a)$ can be thought of as the load of deleterious mutations as considered in classical population genetic models of mutation accumulation (e.g., Kimura and Maruyama, 1966; Haigh, 1978; Dawson, 1999; Bürger, 2000), but here extended to an age-structured model (see also Steinsaltz et al., 2005 for aged-structured mutation accumulation model). As such, we assume that for each age, $n_{\mathrm{m}}(a)$ belongs to the set of non-negative integers ($n_{\mathrm{m}}(a) \in \mathbb{N}$) and

$n_{\mathrm{m}} = \{n_{\mathrm{m}}(a)\}_{a\in\mathcal{T}}$ represents the profile of deleterious mutations across lifespan (formally, n_{m} is thus an element of the space $\mathbb{N}[\mathcal{T}]$ of all possible profiles of range $\mathbb{N}$ and domain $\mathcal{T}$).

From a population genetics perspective, we envision that the genotype of an individual determining the multidimensional trait $\theta = (\boldsymbol{u}, n_{\mathrm{m}})$ consists of two separate positions (or loci) that are necessarily linked under asexual reproduction. One locus determines the number n_{m} of deleterious mutations in the germline. We do not consider the genetic details of this locus, which under sexual reproduction may itself consist of many underlying loci (e.g., Kimura and Maruyama, 1966; Dawson, 1999). The second locus determines the life-history trait(s) and has its own mutation rate independent from the first locus. Furthermore, we assume that to each distinct trait $\boldsymbol{u} \in \mathcal{U}[\mathcal{T}]$ we can associate a distinct haplotype (or allele). We thus assume a separation between genes coding for the life-history trait and those coding for mutation accumulation (see Fig. 1). Conceptually, this is equivalent to the separation between *modifier locus* and loci affecting vital rates of modifier theory, where the modifier locus affects the pattern of transmission of other traits (e.g., Altenberg, 2009). Hence the locus of the life-history trait in our model can be regarded as the modifier locus.

We assume that the effective number of births $b(a)$, the death rate $d(a)$, and the rate $\mu(a)$ of acquiring new germline mutations of an individual of age a can all depend on both $\boldsymbol{u}(a)$ and $n_{\mathrm{m}}(a)$. The life history schedule $\boldsymbol{u}$ thus not only affects the vital rates, as usually assumed in life-history theory, but also the rate of deleterious mutation accumulation (see also Fig. 1). The vital rates may further depend on properties of the population, such as age class densities and allele frequencies, but we leave this dependence implicit for now. We note that when measured on an exponential scale, the death and mutation rates define a survival probability $\exp(-d(a))$ and a immutability probability $\exp(-\mu(a))$ (probability that no mutations occur in an individual of age a). Note that for a discrete time process the birth function $b(a)$ gives the expected number of offspring produced by an individual of age a, while for a continuous time process $b(a)$ is defined as the rate at which an individual produces a single offspring. Finally, we make the following *mutational monotonicity assumption*, which will be central in our analysis.

1. Mutations at the locus for trait n_{m} can only be deleterious or neutral. The effective birth rate $b_i(a)$, survival probability $\exp(-d_i(a))$, and immutability probability $\exp(-\mu_i(a))$ of an individual at age a with $n_{\mathrm{m}}(a) = i$ mutations are non-increasing functions of the number of mutations. Formally, $b_i(a) \geq b_{i+1}(a)$, $d_i(a) \geq d_{i+1}(a)$, and $\mu_i(a) \geq \mu_{i+1}(a)$.

2. Mutations can only accumulate. There are no back mutations and an individual with i mutations can only mutate towards having $i+1$ mutations.

We are concerned in this paper with formalising selection at the life-history locus and not with selection among the entire set of possible genotypes (whose space must code for traits on the daunting cartesian product $\mathcal{U}[\mathcal{T}] \times \mathbb{N}[\mathcal{T}]$). Namely, the objective of our analysis is to develop a tractable evolutionary invasion analysis to evaluate candidate evolutionary stable life-history trait $u^* \in \mathcal{U}[\mathcal{T}]$ that will be favoured by long-term evolution.

2.2 Invasion analysis for life-history with mutation accumulation

2.2.1 Invasion analysis

Evolutionary invasion analysis (e.g., Eshel and Feldman, 1984; Parker and Maynard Smith, 1990; Metz et al., 1992; Charlesworth, 1994; Ferrière and Gatto, 1995; Eshel, 1996; Otto and Day, 2007; Mullon et al., 2016) could be applied straightforwardly to our model in the absence of deleterious mutations as follows. Mutations at the life-history trait are postulated to be very rare so that one can focus on the invasion fitness $\rho(\boldsymbol{u}, \boldsymbol{v})$ of a mutant trait $\boldsymbol{u}$ introduced at low frequency in a population monomorphic for some resident life-history trait $\boldsymbol{v}$ that has reached its demographic equilibrium. The invasion fitness is the per capita number of mutant copies produced per unit time by the mutant lineage descending from the initial mutation, when the mutant reproductive process has reached stationarity in a resident population and remains overall rare (i.e. geometric growth ratio). Traits that are resistant to invasion define candidate end-points of evolution and are found by maximising the invasion fitness of the mutant holding the resident at the uninvadable population state. In others words, an uninvadable trait $\boldsymbol{u}^*$ is a best response to itself; namely

$$\boldsymbol{u}^* \in \arg\max_{\boldsymbol{u} \in \mathcal{U}[\mathcal{T}]} \rho(\boldsymbol{u}, \boldsymbol{u}^*), \tag{1}$$

so that in the resident population state $\boldsymbol{u}^*$, no unilateral trait deviation can increase invasion fitness.

This procedure to characterise stable life histories has been in use more or less explicitly in standard life-history theory for decades (e.g., Michod, 1979; Schaffer, 1982; Iwasa and Roughgarden, 1984; Perrin, 1992; Charlesworth, 1994). We now push forward this approach into the realm where life-history evolution interacts with mutation accumulation and thus relax the assumption that the mutation rate of deleterious mutations is zero. For this case, we still assume that mutations at the life-history loci are rare enough so that whenever a mutant trait $\boldsymbol{u}$ arises, it does so in a resident population monomorphic for some resident life-history trait $\boldsymbol{v}$. But owing to the occurrence of deleterious mutations, the resident population will be polymorphic for the number of deleterious mutations, and this polymorphism will depend on $\boldsymbol{v}$. The resident population is then assumed to have reached a mutation-selection equilibrium for deleterious mutations and the resident trait $\boldsymbol{v}$ thus determines a resident probability distribution $\mathbf{p}(\boldsymbol{v})$ over the different number of deleterious mutations carried by individuals across the different age-classes (the sample space of $\mathbf{p}(\boldsymbol{v})$ is the cartesian product $\mathbb{N} \times \mathcal{T}$). This assumption is nothing else than the assumption of the internal stability of the resident population used in modifier theory (see e.g. Altenberg et al., 2017) or genetically and ecologically minded invasion analysis (see e.g. Eshel and Feldman, 1984; Metz et al., 1992). Here, it entails that the resident population has reached an equilibrium for demographic and genetic processes.

In the absence of age-classes, $\mathbf{p}(\boldsymbol{v})$ is akin to the equilibrium probability distribution for the number of deleterious mutations in standard selection-mutation balance models (see Bürger, 2000 for a general treatment and where the sample space of $\mathbf{p}(\boldsymbol{v})$ reduces to $\mathbb{N}$). For instance, when the number of novel

(deleterious) mutations follows a Poisson distribution with mean rate μ and each additional mutation decreases baseline fecundity by a constant multiplicative factor σ in a semelparous population, then $\mathbf{p}(\boldsymbol{v})$ is Poisson distributed with mean μ/σ (Haigh, 1978, Bürger, 2000, p. 300). This holds in an age-structured population across age-classes under certain but limited number of conditions (Steinsaltz et al., 2005). More generally, $\mathbf{p}(\boldsymbol{v})$ will depend on the details of the model.

2.2.2 Invasion process with mutation accumulation

Since the mutant trait $\boldsymbol{u}$ can arise in individuals carrying different numbers of deleterious mutations, the invasion process of $\boldsymbol{u}$ is contingent on the genetic background in which it arises, and we refer to the initial carrier of the $\boldsymbol{u}$ trait as the progenitor (or ancestor) of $\boldsymbol{u}$. The invasion fitness of $\boldsymbol{u}$ is then determined by the size of the lineage of the progenitor, which consists of all of its descendants carrying $\boldsymbol{u}$ far into the future. Namely, the immediate descendants of the progenitor including the surviving self, the immediate descendants of the immediate descendants, etc., covering the whole family history tree *ad infinitum*. Crucially, descendants may accumulate deleterious mutations during the process of initial growth or extinction of the mutant lineage when this lineage is rare (referred to throughout as the "invasion process"). As such, the invasion process can be regarded as a multitype age-dependent branching process (Mode, 1968, 1971) since during growth or extinction, novel genotypes are produced by mutation. To analyse this process, it is useful to organise individuals into *equivalence classes*. The defining feature of an equivalence class is that it is a collection of states of a process among which transitions eventually occur, so the states are said to communicate (Karlin and Taylor, 1975, p. 60). The equivalence class $\mathcal{C}_i$ will stand for all mutant individuals carrying i deleterious mutations and thus consist of individuals of all age classes. This is an equivalence class because through survival and reproduction, an individual of any age with i mutation may eventually transition to become an individual of any other age (in the absence of menopause). This follows from the fact that the process of survival and reproduction in an age-structured population in the absence of mutations (and menopause) is irreducible because starting in any age-class, eventually every age-class can be reached (Caswell, 2000). Owing to the mutational monotonicity assumption, however, starting in a given class, it is possible to enter another class, but not transition back from that class (otherwise the two class would form a single class) and so the mutant population process is overall reducible. We say that equivalence class $\mathcal{C}_{i+1}$ follows class $\mathcal{C}_i$ since individuals in equivalence class i can only transition to class $i+1$ by acquiring mutations.

To see why the notion of equivalence class is useful to understand the invasion process, let us focus on a discrete time process with discrete age classes; namely, $\mathcal{T} = \{0, 1, 2, ..., T\}$ and we denote by $n_i(t)$ the expected number of individuals at time t in class $\mathcal{C}_i$ that descend from a single class $\mathcal{C}_i$ newborn ancestor born t time-units ago (i.e. $n_i(0) = 1$). Then, accounting for all the descendants of the progenitor (including the surviving self) entails that $n_i(t)$ satisfies the renewal equation

$$n_i(t) = \tilde{l}_i(t) + \sum_{a=0}^{t} n_i(t-a)\tilde{b}_i(a)\tilde{l}_i(a), \tag{2}$$

where $\tilde{l}_i(a)$ is the probability that a $\mathcal{C}_i$ class newborn survives to age a and has not acquired any new mutations (we assume that $\tilde{l}_i(a) \to 0$ as $a \to \infty$, since mutation or death is inevitable eventually). The quantity $\tilde{b}_i(a)$ is the expected number of (newborn) offspring without new mutations produced by an individual of age a that carries i deleterious mutations. Hence, the first term on the right-hand-side of eq. (2) accounts for the survival and immutability of the ancestor itself until age t, while the second term projects the expected number of newborns without mutations descending from the progenitor until time t into its total lineage members without mutation at t. A key feature of eq. (2) is that it depends only on the vital rates and states of individuals of class $\mathcal{C}_i$. As such, eq. (2) is functionally equivalent to the standard renewal equation of population dynamics in discrete age-structured populations (Charlesworth, 1994, eq. 1.34). It then follows from standard results (e.g., Charlesworth, 1994, p. 25-26) that asymptotically, as $t \to \infty$, the number $n_i(t)$ grows geometrically as

$$n_i(t) \sim \rho_i^t K_i, \tag{3}$$

where K_i is a some constant depending on the process and ρ_i is the unique root satisfying the characteristic (or Euler-Lotka) equation $\sum_{a=0}^{T} \rho_i^{-a} \tilde{l}_i(a)\tilde{b}_i(a) = 1$.

Since the equivalence class $\mathcal{C}_{i+1}$ follows class $\mathcal{C}_i$, $n_i(t)$ does not describe the total expected lineage size of the progenitor, since such individuals will contribute to individuals of class $i+1$ through mutations. Owing to the mutational monotonicity assumption, however, the growth ratio ρ_i is at least as large as ρ_{i+1}, i.e., $\rho_i \geq \rho_{i+1}$. This implies that when the ancestor is of type i, the expected lineage size is determined by the growth ratio ρ_i, since it dominates that of any other following equivalence class. Hence, asymptotically, the total expected lineage of an $\mathcal{C}_i$ class progenitor has geometric growth ratio ρ_i. It further follows from the theory of multitype age-dependent branching processes that the realised lineage size of a single progenitor (a random variable) has growth ratio ρ_i if $\rho_i > 1$ and otherwise it goes extinct with probability one (Mode, 1971, Theorem 7.2 p. 245, Corrolary 6.1 p. 280, see also Mode, 1968 for the single type case). Further, $\rho_i \leq 1$ if (and only if) $\tilde{R}_i \leq 1$, where $\tilde{R}_i = \sum_{a=0}^{T} \tilde{l}_i(a)\tilde{b}_i(a)$ is the expected number of offspring of the progenitor produced throughout its lifespan (i.e. Mode, 1971, Theorem 7.2 p. 245, Corrolary 6.1 p. 280, see also Karlin and Taylor, 1981, p. 424, Caswell, 2000). Hence, ρ_i is an appropriate measure of invasion fitness and $\tilde{R}_i$ is an appropriate proxy of it, for a type i mutant $\boldsymbol{u}$ arising in an resident $\boldsymbol{v}$ background (for a discussion of various biological representations of invasion fitness and proxies thereof see Lehmann et al., 2016). The same argument can be made for continuous time processes, in which case $\rho_i = \exp(r_i)$, where r_i is the rate of natural increase of the lineage size of a progenitor of type i, i.e., the Malthusian growth rate (see Appendix A).

2.3 Uninvadability for dominating least loaded class

The key feature of the invasion process in a population with distinct mutational equivalence classes is that the invasion of a mutant depends on the class in which it appears (ρ_i for class i), which in turn

depends on the distribution $\mathbf{p}(\boldsymbol{v})$. This means that there are as many growth rates as equivalence classes, since the invasion process is reducible (see also Altenberg, 2009, p. 1278). Therefore characterising long-term evolution using a single representation of invasion fitness seems unattainable under our modelling assumptions. Yet, as a first-step, it also seems reasonable to assume that the mutation-selection process is such that the least-loaded class $\mathcal{C}_0$ dominates the population in frequency (i.e. the frequency of the zero-class individuals is close to one). For instance, if selection is much stronger than mutation, then deleterious alleles will tend to be purged and the mutation-selection balance will be far away from the error threshold of mutation accumulation or meltdown of asexual population (e.g., Eigen, 1971; Lynch et al., 1993; Szathmary and Maynard Smith, 1997). In this case, whenever a mutant life-history trait $\boldsymbol{u}$ appears in a resident $\boldsymbol{v}$ population, it is most likely to spread on a zero mutation background (i.e. in class $\mathcal{C}_0$ individuals). This assumption is rooted in the argument of Fisher (1930) who remarked that in asexual populations "it will only be the best adapted genotypes which can become the ancestors of future generations, and the beneficial mutations which occur will have only the minutest chance of not appearing in types of organisms so inferior to some of their competitors, that their offspring will certainly be supplanted by those of the latter" (Fisher, 1930, p. 122). Fisher's argument was also implicitly assumed by Dawson (1999, p. 9) to study direct selection on a mutation modifier and we are endorsing it here as it allows to characterise uninvadability (recall eq. 1) directly from the growth ratio

$$\rho(\boldsymbol{u},\boldsymbol{v}) = \rho_0(\boldsymbol{u},\boldsymbol{v}), \tag{4}$$

of the least-loaded class. Further, since $\rho_0(\boldsymbol{u},\boldsymbol{v}) \leq 1 \iff \tilde{R}_0(\boldsymbol{u},\boldsymbol{v}) \leq 1$, where $\tilde{R}_0(\boldsymbol{u},\boldsymbol{v})$ is the basic reproductive number of the least-loaded class, i.e. the expected number of class $\mathcal{C}_0$ offspring produced by a class individual $\mathcal{C}_0$ individual over its lifespan, is sufficient to characterise uninvadability.

It therefore follows that if the least-loaded class dominates in frequency the resident population, an uninvadable strategy $\boldsymbol{u}^*$ can be characterised in a discrete age-structured population as

$$\boldsymbol{u}^* \in \arg\max_{\boldsymbol{u}\in\mathcal{U}[\mathcal{T}]} \tilde{R}_0(\boldsymbol{u},\boldsymbol{u}^*), \tag{5}$$

which entails maximising (in the best response sense) the basic reproductive number of the least-loaded class. This number is given explicitly in terms of vital rates by

$$\tilde{R}_0(\boldsymbol{u},\boldsymbol{v}) = \sum_{a=0}^{T} \tilde{b}_0(a,\boldsymbol{u},\boldsymbol{v})\tilde{l}_0(a,\boldsymbol{u},\boldsymbol{v}), \tag{6}$$

where

$$\tilde{b}_0(a,\boldsymbol{u},\boldsymbol{v}) = b_0(a,\boldsymbol{u},\boldsymbol{v}) \times \exp\left(-\mu_{\mathrm{f}}(a,\boldsymbol{u},\boldsymbol{v})\right) \tag{7}$$

and

$$\tilde{l}_0(a,\boldsymbol{u},\boldsymbol{v}) = l_0(a,\boldsymbol{u},\boldsymbol{v}) \times \exp\left(-\sum_{t=0}^{a-1}\mu_{\mathrm{s}}(t,\boldsymbol{u},\boldsymbol{v})\right) \quad \text{with} \quad l_0(a,\boldsymbol{u},\boldsymbol{v}) = \prod_{t=0}^{a} s_0(t,\boldsymbol{u},\boldsymbol{v}). \tag{8}$$

Here, $b_0(a,\boldsymbol{u},\boldsymbol{v})$ is the effective fecundity of an individual of age a who has no mutations, $s_0(a,\boldsymbol{u},\boldsymbol{v}) = \exp\left(-d_0(a,\boldsymbol{u},\boldsymbol{v})\right)$ is the probability that such an individual survives over the time interval $[a, a+1]$ (and $d_0(a,\boldsymbol{u},\boldsymbol{v})$ is its death rate), and $l_0(a,\boldsymbol{u},\boldsymbol{v})$ is the probability of survival to age a. In eqs. (7)–(8), we have distinguished between the mutation rate during reproduction $\mu_{\mathrm{f}}(a,\boldsymbol{u},\boldsymbol{v})$, which is the rate at which mutations accumulate in the newborn offspring while the parent giving birth is of age t, and the mutation rate during lifespan $\mu_{\mathrm{s}}(t,\boldsymbol{u},\boldsymbol{v})$, which is the rate at which germline mutations accumulate in an organism of age t. Note that the vital rates $b_0(a,\boldsymbol{u},\boldsymbol{v})$ and $s_0(a,\boldsymbol{u},\boldsymbol{v})$ depend on the resident population and can thus be possibly affected by density-dependent regulation. When $\mu_{\mathrm{f}}(a,\boldsymbol{u},\boldsymbol{v}) = \mu_{\mathrm{s}}(t,\boldsymbol{u},\boldsymbol{v}) = 0$ for all $t \in \mathcal{T}$, eq. (6) reduces to the standard basic reproductive number for age-structured populations (e.g. Charlesworth, 1994). We emphasise that we allowed for fecundity, survival and mutation rate to be dependent on the whole life history schedule because the evolving traits may affect physiological state variables (e.g. body size). Furthermore, individuals can also be affected by the state variables of other individuals (i.e. maternal effects) and hence our formulation implicitly covers these situations and frequency-dependent interactions more generally.

For a continuous time process with a continuous age structure ($\mathcal{T} = [0,T]$), we show in Appendix A that the basic reproductive number of the least-loaded class is

$$\tilde{R}_0(\boldsymbol{u},\boldsymbol{v}) = \int_0^T \tilde{b}_0(a,\boldsymbol{u},\boldsymbol{v})\tilde{l}_0(a,\boldsymbol{u},\boldsymbol{v})\,\mathrm{d}a, \tag{9}$$

where $\tilde{b}_0(a,\boldsymbol{u},\boldsymbol{v})$ takes the same functional form as in eq. (7) but is now interpreted as the effective birth rate (of offspring with no mutations) at age a, and $\tilde{l}(a,\boldsymbol{u},\boldsymbol{v})$ satisfies the differential equation:

$$\frac{\mathrm{d}\tilde{l}_0(a,\boldsymbol{u},\boldsymbol{v})}{\mathrm{d}a} = -\left[d_0(t,\boldsymbol{u},\boldsymbol{v}) + \mu_{\mathrm{s}}(t,\boldsymbol{u},\boldsymbol{v})\right]\tilde{l}_0(a,\boldsymbol{u},\boldsymbol{v}) \quad \text{subject to} \quad \tilde{l}_0(0,\boldsymbol{u},\boldsymbol{v}) = 0. \tag{10}$$

We now make four observations on the use of $\tilde{R}_0(\boldsymbol{u},\boldsymbol{v})$ to characterise long-term coevolution for life-history traits and mutation rates.

(1) Because $\tilde{R}_0(\boldsymbol{u},\boldsymbol{v})$ depends on the amount of deleterious mutations in the population solely via $\boldsymbol{v}$, then the distribution $\mathbf{p}(\boldsymbol{v})$ is needed only under frequency-dependent selection. This makes life-history evolution in the presence of deleterious mutations tractable even if the underlying evolutionary process of mutation is not (see section eq. 3.2 for an example). The characterisation of uninvadability using $\tilde{R}_0(\boldsymbol{u},\boldsymbol{v})$ (and thus applying eqs. 4–10) generalises the results of Dawson (1998, p. 148) to overlapping generations and an explicit life-history context.

(2) Because $\tilde{R}_0(\boldsymbol{u}, \boldsymbol{v})$ takes the standard form of the basic reproductive number, the results of optimal control control and dynamic game theory can be applied to characterise uninvadability. This is useful in particular for reaction norm and developmental evolution and formalising different modes of trait expressions (see Avila et al., 2021).

(3) While low mutation rates are presumed to be able to use $\tilde{R}_0(\boldsymbol{u}, \boldsymbol{v})$, these mutation rates are endogenously determined by the uninvadable strategy. It is thus plausible that the uninvadable mutation rate generally entails low mutation rate. So the assumption of low mutation rate may not appear so drastic and the extent to which this assumptions is limiting depends on considering explicit evolutionary scenarios.

(4) If deleterious mutations are such that all the ρ_i's are proportional to ρ_0's, which is the case for the standard mutation accumulation models with multiplicative effect of (deleterious) mutations, then using $\tilde{R}_0$ does no rely on making the assumption of weak mutations, since regardless in which background the mutation appears, it will grow proportionally to ρ_0, and so if $\tilde{R}_0$ is maximised (in the best response sense) so will ρ_0.

For these reasons, it is appropriate to explore life-history and mutation accumulation coevolution by using $\tilde{R}_0(\boldsymbol{u}, \boldsymbol{v})$ as a proxy of invasion fitness. For the sake of argument, suppose that the least-loaded class $\mathcal{C}_0$ is not dominating the population in frequency and thus we need to consider the different backgrounds (the $\mathcal{C}_i$ classes for $i > 1$) in which mutation may arise. This forces us to consider an evolutionary process where the lineage of the mutant $\boldsymbol{u}$ may transition between the different $\mathcal{C}_i$ and so the evolutionary process itself occurs on a single equivalence class and is irreducible. There are at least three ways this can be formally achieved by maintaining the gist of our modelling assumptions. First, one could introduce a small but non-zero mutation rate at the life-history trait (or locus) to consider explicitly the full evolutionary process, which now becomes irreducible since all states (of the space $\mathcal{U}[\mathcal{T}] \times \mathbb{N}[\mathcal{T}]$) communicate (this is exactly what naturally occurs if one where to do individual-based simulations of the process). Then, one could seek to analyse the trait-substitution sequence of life-history traits in the space $\mathcal{U}[\mathcal{T}]$, by way of deriving a master equation for the probability density $\phi(\boldsymbol{u})$ that the population finds itself in state $\boldsymbol{u}$ to attempt to characterise the stochastically stables states of the evolutionary process (Van Cleve and Lehmann, 2013; Van Cleve, 2015). Second, one could relax the assumption of no back-mutations at the deleterious allele locus, which again results in all states communicating and the process becomes irreducible. Third, one may relax the assumptions of asexual reproduction and allow for recombination to occur, which also results in the underlying process to become irreducible.

The proper formalisation of these cases is relevant for future work, but is likely to result in more complicated formalisations to characterise long-term evolution. As such, in the rest of this paper we consider two scenarios of life-history and mutation accumulation coevolution that we analyse by using $\tilde{R}_0(\boldsymbol{u}, \boldsymbol{v})$. This allows us to illustrate the different concepts, demonstrate the usefulness of first focusing on $\tilde{R}_0(\boldsymbol{u}, \boldsymbol{v})$ to get insights about how life-history evolution interacts with mutation accumulation, and

check results against individual-based simulations.

3 Examples of life-history and mutation rate coevolution

3.1 Coevolution of reproductive effort and the mutation rate

3.1.1 Biological scenario

Our first scenario considers the evolution of reproductive effort when resources can be allocated to (germline) repair in an iteroparous population. To that end, we assume a population with a large but fixed number N of individuals undergoing the following discrete time life-cycle. (1) Each of the N adult individuals produces a large number of juveniles and either survives or dies independently of other individuals. Juveniles and surviving adults acquire mutations at the deleterious allele locus at the same rate. (2) Density-dependent competition occurs among juveniles for the vacated breeding spots (left by the dead adults) and the population is regulated back to size N.

We postulate that individuals have a static life-history trait consisting of two components $\boldsymbol{u} = (u_{\mathrm{r}}, u_{\mathrm{s}})$ ($\boldsymbol{u} \in \mathcal{U}[\mathcal{T}] = [0,1]^2$), which determines how a fixed amount of resources available to each individual is allocated between three physiological functions: (i) a proportion $(1-u_{\mathrm{r}})(1-u_{\mathrm{s}})$ of resources is allocated to reproduction, (ii) a proportion $(1-u_{\mathrm{r}})u_{\mathrm{s}}$ of resources is allocated to survival, and (iii) a proportion u_{r} of resources is allocated to lowering the mutation rate.

We assume that an individual with trait $\boldsymbol{u}$ and i deleterious mutations has the following fecundity, survival probability, and mutation rates (at giving birth and during ageing),

$$\begin{aligned} f_i(\boldsymbol{u}) &= f_0(\boldsymbol{u}) \times (1-\sigma_{\mathrm{f}})^i \\ s_i(\boldsymbol{u}) &= s_0(\boldsymbol{u}) \times (1-\sigma_{\mathrm{s}})^i \\ \mu(\boldsymbol{u}) &= \mu_{\mathrm{s}}(\boldsymbol{u}) = \mu_{\mathrm{f}}(\boldsymbol{u}) = \mu_{\mathrm{b}}\,(1-u_{\mathrm{r}})^{\alpha_\mu}\,, \end{aligned} \tag{11}$$

where σ_{f} and σ_{s} are, respectively, reductions in fecundity and survival from carrying an additional deleterious mutations, μ_{b} is the baseline mutation rate (mutation rate when allocation to germline repair is at its minimum, $u_{\mathrm{r}} = 0$), and α_μ is the repair scaling factor (a parameter tuning how investing a unit resource into repair translates into reducing the mutation rate). We assume that $\alpha_\mu > 1$, such that $\mu(\boldsymbol{u})$ has decreasing negative slopes in u_{r} and hence exhibits diminishing returns from investment into repair. The parameter α_μ can thus be interpreted as the "efficiency" of converting resources to lowering the mutation rates (since higher values of α_μ correspond to lower mutation rates).

The quantities $f_0(\boldsymbol{u})$ and $s_0(\boldsymbol{u})$ are, respectively the fecundity and survival of the least-loaded class and they are written as

$$\begin{aligned} f_0(\boldsymbol{u}) &= f_{\mathrm{b}}\Big((1-u_{\mathrm{s}})(1-u_{\mathrm{r}})\Big)^{\alpha_{\mathrm{f}}} \\ s_0(\boldsymbol{u}) &= s_{\mathrm{b}}\Big(u_{\mathrm{s}}(1-u_{\mathrm{r}})\Big)^{\alpha_{\mathrm{s}}}. \end{aligned} \tag{12}$$

Here, f_{b} and s_{b} are, respectively, the baseline fecundity and survival rate; α_{f} and α_{s} are, respectively, the fecundity and survival scaling factors (parameters tuning how a unit resource translates into fecundity and survival). We assume that $\alpha_{\mathrm{f}}, \alpha_{\mathrm{s}} \leq 1$ whereby both survival and fecundity have decreasing positive slopes in net amount of resources allocated to them and thus exhibit diminishing returns. Since higher values of α_{f} and α_{s} correspond to lower values of fecundity $f_0(\boldsymbol{u})$ and survival $s_0(\boldsymbol{u})$ (keeping everything else constant), we can interpret α_{f} and α_{s} as "inverse efficiencies" of converting resources to vital rates. In the absence of mutation rate, the model reduces to the standard model of reproductive effort of life-history theory with trade-off between reproduction and survival (Charnov, 1993; Pen, 2000; Case, 2000). Conversely, with no survival and no life-history evolution, the model reduces to the classical model of mutation accumulation (Haigh, 1978; Bürger, 2000), and with zero survival and resource allocation evolution, it is equivalent to the asexual model of Dawson (1998). The model thus combines an unexplored trade-off between life-history traits (survival and reproduction) and immutability (germline maintenance and repair).

3.1.2 Basic reproductive number

From the model assumptions, we have that the survival of the least-loaded class (eq. 8) reduces to

$$\tilde{l}_0(a, \boldsymbol{u}, \boldsymbol{v}) = s_0(\boldsymbol{u})^a \exp\left(-\mu(\boldsymbol{u})a\right) \tag{13}$$

and the effective fecundity of the least-loaded class (eq. 7) can be written as

$$\tilde{b}_0(a, \boldsymbol{u}, \boldsymbol{v}) = \tilde{b}_0(\boldsymbol{u}, \boldsymbol{v}) = \underbrace{\left(1 - \bar{s}(\boldsymbol{v})\right) \frac{f_0(\boldsymbol{u})}{\bar{f}(\boldsymbol{v})}}_{b_0(\boldsymbol{u},\boldsymbol{v})} \exp\left(-\mu(\boldsymbol{u})\right), \tag{14}$$

which depends on the mean survival and fecundity in the population, respectively, $\bar{s}(\boldsymbol{v}) = \sum_{k=0}^{\infty} s_k(\boldsymbol{v}) p_k(\boldsymbol{v})$ and $\bar{f}(\boldsymbol{v}) = \sum_{k=0}^{\infty} f_k(\boldsymbol{v}) p_k(\boldsymbol{v})$. Here, $p_i(\boldsymbol{v})$ is the probability that an individuals randomly sampled from the resident population carries i deleterious mutations (and so $\mathbf{p}(\boldsymbol{v}) = \{p_i(\boldsymbol{v})\}_{i \in \mathbb{N}}$ for this model). This can be understood by noting that $(1 - \bar{s}(\boldsymbol{v}))$ is the fraction of open breeding spots available to a juvenile and the probability that the offspring of a given adult acquires a breeding spot depends on the fecundity of the adult relative to the population average fecundity (as each juvenile is equally likely to acquire a breeding spot).

Since there is no fixed end to lifepan under the above life-cycle assumptions (so $T \to \infty$) and using eq. (6) along with eqs. (13)–(14) entails that

$$\tilde{R}_0(\boldsymbol{u}, \boldsymbol{v}) = \frac{b_0(\boldsymbol{u}, \boldsymbol{v})}{\exp(\mu(\boldsymbol{u})) - s_0(\boldsymbol{u})}, \tag{15}$$

(all our mathematical computations can be followed and confirmed via an accompanying Supplementary Material (SM) consisting of a Mathematica Notebook). Since $b_0(\boldsymbol{u}, \boldsymbol{v})$ is multiplicatively separa-

ble with respect to its arguments then it follows from eq. (15) that the model satisfies the condition of an optimisation principle (e.g., Metz et al., 2008). Namely, the basic reproductive number is multiplicatively separable with respect to its arguments, i.e. $\tilde{R}_0(\boldsymbol{u},\boldsymbol{v}) = F_1(\boldsymbol{u})F_2(\boldsymbol{v})$ for the functions $F_1(\boldsymbol{u}) = f_0(\boldsymbol{u})/[\exp(\mu(\boldsymbol{u})) - s_0(\boldsymbol{u})]$, and $F_2(\boldsymbol{v}) = [1-\bar{s}(\boldsymbol{v})]/\bar{f}(\boldsymbol{v})$. It follows that maximising $F_1(\boldsymbol{u})$ is sufficient to ascertain uninvadability and that the explicit expressions for $\bar{s}(\boldsymbol{v})$ and $\bar{f}(\boldsymbol{v})$, and thus the distribution $\mathbf{p}(\boldsymbol{v})$, are not needed to carry out the invasion analysis. We will nevertheless work out the resident distribution $\mathbf{p}(\boldsymbol{v})$ so as to have a fully worked example that allows for consistency checks and illustrating the concepts.

Since we consider a deterministic resident population process, the frequencies p_i satisfy at equilibrium the equation

$$p_k(\boldsymbol{v}) = \sum_{i=0}^{k} \phi_{k-i}(\boldsymbol{v}) w_i(\boldsymbol{v}) p_i(\boldsymbol{v}), \tag{16}$$

where $w_i(\boldsymbol{v}) = s_i(\boldsymbol{v}) + (1-\bar{s}(\boldsymbol{v}))\, f_i(\boldsymbol{v})/\bar{f}(\boldsymbol{v})$ is the individual fitness– survival plus effective fecundity–of an individual with i deleterious mutations, and ϕ_k is the probability that k deleterious mutations are produced upon reproduction. Assuming that the mutation distribution is Poisson with mean $\mu(\boldsymbol{v})$ and $\sigma_{\mathrm{s}} = \sigma_{\mathrm{f}} = \sigma$, then eq. (16) becomes structurally equivalent to eq. (1) of Haigh (1978) and eq. (5.3) of Bürger (2000, p. 300) (with mean fitness $\bar{w} = 1$ since population size is constant) and as such the equilibrium distribution $\mathbf{p}(\boldsymbol{v})$ is Poisson with mean $\lambda(\boldsymbol{v}) = \mu(\boldsymbol{v})/\sigma$ (see also the section 1.1.1. in SM). This completely characterises the genetic state of the resident population and implies that

$$\bar{s}(\boldsymbol{v}) = s_0(\boldsymbol{v})e^{-\mu(\boldsymbol{v})} \quad \text{and} \quad \bar{f}(\boldsymbol{v}) = f_0(\boldsymbol{v})e^{-\mu(\boldsymbol{v})}. \tag{17}$$

Substituting the explicit expression for the survival and effective fecundities (eq. 17) into eq. (15) shows that in a monomorphic $\boldsymbol{v}$ population $\tilde{R}_0(\boldsymbol{v},\boldsymbol{v}) = 1$, as required for a consistent model formulation.

3.1.3 Uninvadable strategies

We now carry out the invasion analysis explicitly following the standard approach of working with selection gradients (e.g., Parker and Maynard Smith, 1990; Frank, 2008; Geritz et al., 1998; Rousset, 2004; Mullon et al., 2016). Using eq. (11), (12), (14), and (17) in eq. (15) and taking the derivative with respect to u_{r}, we find that the selection gradient on repair can be written as

$$\left.\frac{\partial \tilde{R}_0(\boldsymbol{u},\boldsymbol{v})}{\partial u_{\mathrm{r}}}\right|_{\substack{u_{\mathrm{r}}=v_{\mathrm{r}}\\ u_{\mathrm{s}}=v_{\mathrm{s}}}} = \frac{1}{(1-\bar{s}(\boldsymbol{v}))\,(1-v_{\mathrm{r}})}\left(\alpha_\mu \mu(\boldsymbol{v}) - \left[\alpha_{\mathrm{s}}\bar{s}(\boldsymbol{v}) + \alpha_{\mathrm{f}}\,(1-\bar{s}(\boldsymbol{v}))\right]\right), \tag{18}$$

where the terms in parenthesis display the trade-off between allocating resources into repair vs. the two vital rates. The first term in eq. (18) is the marginal benefit of investment into repair, which is a decreasing function of v_{r}. The second term is the marginal cost of investment into repair and this

depends on the weighted sum over average survival and open breeding spots and is a concave function of v_r if $\alpha_\mathrm{s} > \alpha_\mathrm{f}$, a convex function of v_r if $\alpha_\mathrm{s} < \alpha_\mathrm{f}$, and independent of v_r if $\alpha_\mathrm{s} = \alpha_\mathrm{f} = \alpha$. Decreasing α_μ corresponds to increasing the mutation rate and decreasing α_s and α_f corresponds to increasing fecundity and survival (holding everything else constant), and for this reason decreasing α_μ, α_s, and α_f favours allocation of resources to repair. We find that the selection gradient on survival can be written as

$$\left.\frac{\partial \tilde{R}_0(\boldsymbol{u},\boldsymbol{v})}{\partial u_\mathrm{s}}\right|_{\substack{u_\mathrm{r}=v_\mathrm{r}\\ u_\mathrm{s}=v_\mathrm{s}}} = \frac{1}{1-\bar{s}(\boldsymbol{v})}\left(\frac{\alpha_\mathrm{s}\bar{s}(\boldsymbol{v})}{v_\mathrm{s}} - \frac{\alpha_\mathrm{f}(1-\bar{s}(\boldsymbol{v}))}{(1-v_\mathrm{s})}\right), \tag{19}$$

where the terms in the parenthesis display the trade-off between allocating resources into survival vs. fecundity. The first term in eq. (19) is the marginal benefit of investments into survival, which is a decreasing function of v_r, while the second term is the marginal benefit of investments into fecundity, and increasing function of v_r. This trade-off is the classical reproductive effort trade-off (e.g., Pen, 2000, eq. 4) with the difference that it is here affected by the mutation rate. In particular, baseline mutation rates $\mu_\mathrm{b}(v_\mathrm{r})$ favours higher allocation to survival (by increasing $\bar{s}(\boldsymbol{v})$).

A necessary condition for $(u_\mathrm{r}^*, u_\mathrm{s}^*) = \boldsymbol{u}^*$ to be uninvadable is that the selection gradients vanish at this point (for an interior equilibrium, i.e. $0 < u_\mathrm{r}^*, u_\mathrm{s}^* < 1$), i.e. $\partial\tilde{R}_0(\boldsymbol{u},\boldsymbol{v})/\partial u_\mathrm{s} = 0$ and $\partial\tilde{R}_0(\boldsymbol{u},\boldsymbol{v})/\partial u_\mathrm{r} = 0$ evaluated at $\boldsymbol{v} = \boldsymbol{u}^*$. Without further assumptions on eqs. (18)–(19), we were unable to find such analytical solutions. But setting $\alpha_\mathrm{s} = \alpha_\mathrm{f} = \alpha$, we find that there is a unique solution

$$u_\mathrm{r}^* = \begin{cases} 0 & \text{if } \mu_\mathrm{b} \le \frac{\alpha}{\alpha_\mu} \\ 1 - \left(\frac{\alpha}{\alpha_\mu \mu_\mathrm{b}}\right)^{\frac{1}{\alpha_\mu}} & \text{otherwise} \end{cases}, \qquad u_\mathrm{s}^* = \begin{cases} \left(\frac{\exp(\mu_\mathrm{b})}{s_\mathrm{b}}\right)^{\frac{1}{\alpha-1}} & \text{if } \mu_\mathrm{b} \le \frac{\alpha}{\alpha_\mu} \\ \left(\frac{\exp(\frac{\alpha}{\alpha_\mu})\left(\frac{\alpha}{\alpha_\mu \mu_\mathrm{b}}\right)^{-\frac{\alpha}{\alpha_\mu}}}{s_\mathrm{b}}\right)^{\frac{1}{\alpha-1}} & \text{otherwise} \end{cases}. \tag{20}$$

Eq. (20) gives the candidate uninvadable strategies, we checked that for biologically realistic parameter values, (e.g. for the parameter values in Fig. 2) these strategies are also uninvadable, using the standard approach of ascertaining uninvability (Eshel, 1983; Taylor, 1989; Geritz et al., 1998; Mullon et al., 2016 and see the SM). While we derived the (candidate) uninvadable strategies $\boldsymbol{u}^* = (u_\mathrm{r}^*, u_\mathrm{s}^*)$ assuming $\alpha_\mathrm{f} = \alpha_\mathrm{s}$, we checked the robustness of the qualitative behaviour of the results with respect to parameter values numerically for $\alpha_\mathrm{f} \neq \alpha_\mathrm{s}$ and we find that overall behaviour of the results remain the same even when $\alpha_\mathrm{f} \neq \alpha_\mathrm{s}$. The corresponding expressions for the mutation rate $\mu(\boldsymbol{u}^*)$ and the mean number of novel (deleterious) mutations $\lambda(\boldsymbol{u}^*)$ take the following form

$$\mu(\boldsymbol{u}^*) = \begin{cases} \mu_\mathrm{b} & \text{if } u_\mathrm{r}^* = 0 \\ \alpha/\alpha_\mu & \text{if } u_\mathrm{r}^* > 0 \end{cases}, \qquad \lambda(\boldsymbol{u}^*) = \begin{cases} \mu_\mathrm{b}/\sigma & \text{if } u_\mathrm{r}^* = 0 \\ \alpha/(\alpha_\mu \sigma) & \text{if } u_\mathrm{r}^* > 0 \end{cases}. \tag{21}$$

Fig. (2) illustrates the uninvadable life-history strategies $\boldsymbol{u}^* = (u_\mathrm{r}^*, u_\mathrm{s}^*)$ (panels a and b), the corresponding mutation rate $\mu(\boldsymbol{u}^*)$ (panel c) and the mean number of novel mutations $\lambda(\boldsymbol{u}^*)$ (panel d) as a function of the baseline mutation rate μ_b. We can observe from Fig. (2) that the analytically obtained results (eq. 20–

21) correspond very closely to those obtained by carrying out individual-based stochastic simulations of the full process, which implements the life-cycle and assumptions of the present biological scenarios but allows for mutation at the life-history locus (e.g. Fig. 1 and see the S.I. file for the Mathematica code for doing the simulations). Overall, three main results can be drawn from Fig. (2) and eqs. (20)–(21).

First, investment into germline repair u_{r}^* is predicted to evolve when baseline mutation rate is high enough ($\mu_{\mathrm{b}} > \frac{\alpha}{\alpha_\mu}$) and when it evolves, allocation to repair u_{r}^* increases with the baseline mutation rate μ_{b} (Fig. 2a). This result also holds when $\alpha_{\mathrm{s}} \neq \alpha_{\mathrm{f}}$ (see numerical calculations in the SM). Investment into repair is higher when resource allocation to vital rates is more "efficient" (α is smaller), but directing resources to lowering the mutation rate is less "efficient" (α_μ is smaller).

Second, the uninvadable mutation rate is a constant $\mu(\boldsymbol{u}^*) = \alpha/\alpha_\mu$ determined by the inverse of resource conversion "efficiencies", when repair evolves ($u_{\mathrm{r}}^* > 0$ and $\mu_{\mathrm{b}} > \frac{\alpha}{\alpha_\mu}$), otherwise the uninvadable mutation rate is equal to the baseline mutation rate $\mu(\boldsymbol{u}^*) = \mu_{\mathrm{b}}$ (see Fig. 2c and eq. 21). It might seem surprising that the uninvadable mutation rate is independent of the baseline mutation rate when repair evolves. To understand this, we note that at the uninvadable state, the marginal benefit of repair $\alpha_\mu \mu(\boldsymbol{u}^*)$ (up to a constant of proportionality) is equal to the marginal cost α (up to a constant of proportionality) of repair, which follows from letting the selection gradient, given by eq. 18 to vanish while taking $\alpha = \alpha_{\mathrm{s}} = \alpha_{\mathrm{s}}$ and $\boldsymbol{v} = \boldsymbol{u}^*$. Thus, the uninvadable mutation rate must be necessarily given by $\mu(\boldsymbol{u}^*) = \alpha/\alpha_\mu$. It is important to notice here that the marginal cost α of repair is here only given by a constant since the effect of mean survival $\bar{s}(\boldsymbol{v})$ that depends on the baseline mutation rate cancels out as $\alpha_{\mathrm{f}} = \alpha_{\mathrm{s}}$. However, we checked numerically that even if $\alpha_{\mathrm{f}} \neq \alpha_{\mathrm{s}}$ and $u_{\mathrm{r}}^* > 0$, then $\mu(\boldsymbol{u}^*)$ still tends to be independent of baseline mutation rate for a wide range of parameter values. Intuitively, this can be explained as follows, the baseline mutation rate μ_{b} does not affect the uninvadable mutation rate, since its affect on the cost of repair via the mean survival $\bar{s}(\boldsymbol{v})$ cancels out. That is, the mutation rate reduces the expected survival, but this effect on fitness is exactly cancelled by the increase in the breeding success (as the number of breeding spots increase due to decrease in survival in the population due to mutation rate).

Third, the survival-reproduction trade-off is shifting towards higher investment into reproduction at the expense of survival as the baseline mutation rate μ_{b} increases (Fig. 2b). This gradual shift towards reproduction with increasing μ_{b} occurs even while the uninvadable mutation rate $\mu(\boldsymbol{u}^*)$ stays constant with μ_{b}. Hence our model indicates that measuring the "observed" mutation rate ($\mu(\boldsymbol{u}^*)$) does not capture the effect of how the process of deleterious mutation accumulation affects life-history trade-offs. Another observation about survival-reproduction trade-off that we can make from eq. (20) is that the absence of external mortality ($s_{\mathrm{b}} = 1$) is not enough for all resources to be allocated to survival and hence immortality (complete survival, $\bar{s}(\boldsymbol{u}^*) = s_0(\boldsymbol{u}^*) = 1$) to evolve. Immortality can evolve in this model only in the absence of external mortality and zero baseline mutations ($s_{\mathrm{b}} = 1$, $\mu_{\mathrm{b}} = 0$). This emphasises that even under "perfect environment" (where external causes of mortality can be eliminated), immortality can not persist due to non-zero mutation rates.

3.2 Coevolution of age of maturity and germline repair coevolution

3.2.1 Biological scenario

Our second scenario is about the evolution of the time at maturity when mutation accumulation can occur during growth and reproduction. To that end, we consider that age is continuous and each individual undergoes the following events. (1) An individual is born and grows in size until it reaches maturity (growth phase). (2) At maturity an individual starts to reproduce at a constant rate and fecundity is assumed to be density dependent (reproductive phase). (3) Throughout their lives individuals die at some constant rate and acquire mutations. We postulate that individuals have again a life-history trait consisting of two components $\boldsymbol{u} = (u_{\mathrm{r}}, u_{\mathrm{m}})$, where u_{r} is the allocation to germline repair (lowering the mutation rate) and u_{m} is the age-at-maturity. The life-history trait $\boldsymbol{u}$ determines how resources are allocated between three physiological functions: (i) a proportion u_{r} of resources is allocated to repair and maintenance of the germline at any age a, (ii) a proportion $(1 - u_{\mathrm{r}})$ of resources are allocated to growth when an individual is of age $a < u_{\mathrm{m}}$, (iii) a proportion $(1 - u_{\mathrm{r}})$ of resources is allocated to reproduction when an individual is at age $a \geq u_{\mathrm{m}}$, (hence $\boldsymbol{u} \in \mathcal{U}[\mathcal{T}] = [0, 1]^2$).

We assume that an individual with trait $\boldsymbol{u}$ and i deleterious mutations in a population with resident trait $\boldsymbol{v}$ has birth, death, and mutation rate throughout lifespan given by

$$\begin{aligned} \tilde{b}_i(\boldsymbol{u}, \boldsymbol{v}) &= \tilde{b}_0(\boldsymbol{u}, \boldsymbol{v}) - i\sigma_{\mathrm{b}} \quad \text{if } a \geq u_{\mathrm{m}}, \text{ zero otherwise} \\ d_i &= d_{\mathrm{b}} + i\sigma_{\mathrm{d}} \\ \mu_{\mathrm{s}}(u_{\mathrm{r}}) &= \mu_{\mathrm{b}}(1 - u_{\mathrm{r}})^{\alpha_\mu}, \end{aligned} \tag{22}$$

where σ_{b} and σ_{d} are, respectively, the effects on birth and death from carrying deleterious. The death rate of an individual of the least-loaded class is determined by the baseline death rate d_{b} and the birth rate of such an individual is assumed to be given by

$$\tilde{b}_0(\boldsymbol{u}, \boldsymbol{v}) = \underbrace{B(x_{\mathrm{m}}(\boldsymbol{u}))(1 - u_{\mathrm{r}}^{\alpha_{\mathrm{b}}})(1 - \gamma N(\boldsymbol{v}))}_{b_0(\boldsymbol{u}, \boldsymbol{v})} \exp(-\mu_{\mathrm{f}}), \tag{23}$$

where $B(x_{\mathrm{m}}(\boldsymbol{u}))$ is the surplus energy, i.e., energy available to considered life-history functions, which depends on the size $x_{\mathrm{m}}(\boldsymbol{u})$ of the individual at maturity. Here, $(1 - u_{\mathrm{r}}^{\alpha_{\mathrm{b}}})$ represents how reproduction depends on the allocation strategy and $u_{\mathrm{r}}^{\alpha_{\mathrm{b}}}$ represents the cost to reproduction when allocating a proportion u_{r} of resources to repair and α_{b} can be loosely interpreted as a parameter tuning the "efficiency" of investing resources into reproduction (higher values of α_{b} correspond to increased reproduction). The term $(1-\gamma N(\boldsymbol{v}))$ accounts for density-dependent regulation of reproduction, where $N(\boldsymbol{v})$ is the total population size of the resident population and γ tunes the intensity of density dependence. Finally, $\exp(-\mu_{\mathrm{f}})$ is the probability that the offspring do not acquire new mutations during reproduction where the mutation rate at giving birth μ_{f} is assumed constant (corresponding to eq. (7) when taking $\mu_{\mathrm{f}} = \mu_{\mathrm{s}}(a, \boldsymbol{u}, \boldsymbol{v})$). In order to close the expression for the birth rate, we need an explicit expression for $x_{\mathrm{m}}(\boldsymbol{u})$. During the

growth phase, we postulate that the size of an individual follows the dynamic equation

$$\dot{x}(t) = \beta B(x(t))(1 - u_{\mathrm{r}}^{\alpha_{\mathrm{b}}}) \qquad \text{with i.c. } x(0) = x_0, \tag{24}$$

where $B(x(t))$ is the surplus energy when an individual is of size $x(t)$, $(1-u_{\mathrm{r}}^{\alpha_{\mathrm{b}}})$ represents the proportional allocation of resources devoted towards growth (instead of repair) and for tractability is assumed to have the form as the proportional allocation towards reproduction (eq. 23) and β allows to tune how much resources are needed to grow one unit, compared to the resources needed to produce one offspring. We assume that the surplus energy is given by the power law $B(x(t)) = ax(t)^c$, which is considered to be appropriate for modelling size/age-at-maturity under determinate growth (see Day and Taylor (1996) for a justification). It follows from integrating eq. (24) that the size at maturity is a function of both life-history traits and takes the following form

$$x_{\mathrm{m}}(\boldsymbol{u}) = \left(\beta a(1-c)(1 - u_{\mathrm{r}}^{\alpha_{\mathrm{b}}})u_{\mathrm{m}} + x_0^{1-c}\right)^{\frac{1}{1-c}}. \tag{25}$$

In the absence of mutation rate, the model reduces to the standard model of age-at maturity Kozlowski, 1992; Day and Taylor, 1997; Stearns, 1992; Roff, 2008. The model thus combines an unexplored trade-offs between life-history traits (growth and reproduction) and immutability (germline maintenance and repair).

3.2.2 Basic reproductive number

For this model there is also no definite end to lifepan (and so $T \to \infty$) and using eq. (9) with the life-cycle assumptions entails that the basic reproductive number of the least-loaded class reduces to

$$\tilde{R}_0(\boldsymbol{u}, \boldsymbol{v}) = \tilde{b}_0(\boldsymbol{u}, \boldsymbol{v}) \int_{u_{\mathrm{m}}}^{\infty} \tilde{l}_0(a, \boldsymbol{u}, \boldsymbol{v})\, \mathrm{d}a, \tag{26}$$

where $\tilde{l}_0(a, \boldsymbol{u}, \boldsymbol{v}) = \exp\Big(-(\mu(u_{\mathrm{r}}) + d_{\mathrm{b}})a\Big)$. Substituting the expression for eq. (23) into eq. (26) and integrating yields

$$\tilde{R}_0(\boldsymbol{u}, \boldsymbol{v}) = \underbrace{B(x_{\mathrm{m}}(\boldsymbol{u}))\,(1 - u_{\mathrm{r}}^{\alpha_{\mathrm{b}}})\exp(-\mu_{\mathrm{f}}) \times \frac{\exp\Big(-(\mu(u_{\mathrm{r}}) + d_{\mathrm{b}})u_{\mathrm{m}}\Big)}{\mu(u_{\mathrm{r}}) + d_{\mathrm{b}}}}_{F_1(\boldsymbol{u})} \times \underbrace{(1 - \gamma N(\boldsymbol{v}))}_{F_2(\boldsymbol{v})}. \tag{27}$$

This shows that one can again express the basic reproductive number as a product of the form $\tilde{R}_0(\boldsymbol{u}, \boldsymbol{v}) = F_1(\boldsymbol{u})F_2(\boldsymbol{v})$ and evaluating $N(\boldsymbol{v})$ explicitly is not needed to ascertain uninvadability. We will nevertheless work it out and in order to derive an explicit expression for $N(\boldsymbol{v})$ it suffices to note that in a monomorphic resident population at a joint demographic and genetic equilibrium, each individual belonging to the least-loaded class must leaves on average one descendant with zero new mutations. Hence $\tilde{R}_0(\boldsymbol{v}, \boldsymbol{v}) = 1$ implies

that at the population size at the demographic steady state is

$$N(\boldsymbol{v}) = \frac{B(x_{\mathrm{m}}(\boldsymbol{v}))(1 - v_{\mathrm{r}}^{\alpha_{\mathrm{b}}}) - (d_{\mathrm{b}} + \mu(v_{\mathrm{r}}))\exp\Big(\mu_{\mathrm{f}} + (\mu(v_{\mathrm{r}}) + d_{\mathrm{b}})v_{\mathrm{m}}\Big)}{\gamma B(x_{\mathrm{m}}(\boldsymbol{v}))(1 - v_{\mathrm{r}}^{\alpha_{\mathrm{b}}})}, \tag{28}$$

which holds regardless of the effects of deleterious mutations on the vital rates. This is a demographic representation and generalisation of the surprising simple result noted for unstructured semelparous populations of constant size that the epistasic effects of deleterious mutations do not affect the genetic load (Kimura and Maruyama, 1966; Gillespie, 2004).

3.2.3 Uninvadable strategies

Let us now ascertain the strategies favored by long-term evolution. Using eq. (27) along with eq. (25), taking the derivative with respect to u_{r}, and rearranging using the property that $\tilde{R}_0(\boldsymbol{v}, \boldsymbol{v}) = 1$, we find that the selection gradient on repair can be written as

$$\left.\frac{\partial \tilde{R}_0(\boldsymbol{u}, \boldsymbol{v})}{\partial u_{\mathrm{r}}}\right|_{\substack{u_{\mathrm{m}}=v_{\mathrm{m}} \\ u_{\mathrm{r}}=v_{\mathrm{r}}}} = \frac{\alpha_{\mu}\mu(v_{\mathrm{r}})}{(1 - v_{\mathrm{r}})}\Big(v_{\mathrm{m}} + \frac{1}{\mu(v_{\mathrm{r}}) + d_{\mathrm{b}}}\Big) - \alpha_{\mathrm{b}} v_{\mathrm{r}}^{\alpha_{\mathrm{b}}-1}\left(\beta\frac{c v_{\mathrm{m}} B(x_{\mathrm{m}}(\boldsymbol{v}))}{x_{\mathrm{m}}(\boldsymbol{v})} + \frac{1}{(1 - v_{\mathrm{r}}^{\alpha_{\mathrm{b}}})}\right), \tag{29}$$

where the two terms display the trade-off between allocating resources into repair vs. growth and reproduction. The first term is the marginal benefit of investing into repair and the second term is marginal cost of investing into repair which is a weighted sum of expected loss in growth and reproduction. We find that the selection gradient on the age-at-maturity can be written as

$$\left.\frac{\partial \tilde{R}_0(\boldsymbol{u}, \boldsymbol{v})}{\partial u_{\mathrm{m}}}\right|_{\substack{u_{\mathrm{m}}=v_{\mathrm{m}} \\ u_{\mathrm{r}}=v_{\mathrm{r}}}} = c \times \frac{\beta\Big(1 - v_{\mathrm{r}}^{\alpha_{\mathrm{b}}}\Big)B(x_{\mathrm{m}}(\boldsymbol{v}))}{x_{\mathrm{m}}(\boldsymbol{v})} - (\mu(v_{\mathrm{r}}) + d_{\mathrm{b}}). \tag{30}$$

The first term is the marginal benefit of investment into growth and thus the benefit for maturing later, while the second terms is the marginal cost of investment into growth and thus the benefit for maturing earlier. We can see that the increase in mutation rate will select for earlier age-at-maturity.

By first solving $\partial \tilde{R}_0(\boldsymbol{u}, \boldsymbol{v})/\partial u_{\mathrm{m}} = 0$ for u_{m}^* when evaluated at $\boldsymbol{v} = \boldsymbol{u} = \boldsymbol{u}^*$, we obtain

$$u_{\mathrm{m}}^*(u_{\mathrm{r}}^*) = \frac{1}{1 - c} \times \left(\frac{c}{d_{\mathrm{b}} + \mu(u_{\mathrm{r}}^*)} - \frac{x_0}{\beta[1 - (u_{\mathrm{r}}^*)^{\alpha_{\mathrm{b}}}]B(x_0)}\right), \tag{31}$$

which is a function u_{r}^*. Eq. (31) says that individuals tends to mature later, when individuals growth rate at birth $\dot{x}(0)$ $(= \beta[1 - (u_{\mathrm{r}}^*)^{\alpha_{\mathrm{b}}}]B(x_0))$ is higher and/or when death rate d_{b}, mutation rate $\mu(u_{\mathrm{r}}^*)$, and birth size x_0 are smaller (holding everything else constant). When $\mu_{\mathrm{b}} \to 0$ and $u_{\mathrm{r}}^* \to 0$, age-at-maturity reduces to $u_{\mathrm{m}}^* = (1 - c)^{-1}[c/d_{\mathrm{b}} - x_0/[\beta a x_0^c]$, which is consistent with standard results about the optimal age/size at maturity (see e.g. Day and Taylor, 1996) and it is useful to compare how allocation to germline repair affects the age-at-maturity. In order to determine a joint equilibrium $\boldsymbol{u}^* = (u_{\mathrm{m}}^*, u_{\mathrm{r}}^*)$, we need to substitute eq. (31) into eq. (30) and solve for u_{m}^* and u_{r}^* at $\boldsymbol{v} = \boldsymbol{u}^*$. We were unable to obtain an analytical solution

for the general case. But restricting attention to $\alpha_\mu = \alpha_\mathrm{b} = 2$, we find that the candidate uninvadable traits are

$$
\begin{aligned}
u_\mathrm{r}^* &= \frac{2\mu_\mathrm{b} + d_\mathrm{b} - \sqrt{d_\mathrm{b}(d_\mathrm{b} + 4\mu_\mathrm{b})}}{2\mu_\mathrm{b}} \\
u_\mathrm{m}^* &= \frac{1}{(1-c)} \times \left[c\Big(\frac{\sqrt{d} + \sqrt{d_\mathrm{b} + 4\mu_\mathrm{b}}}{2d_\mathrm{b}\sqrt{d_\mathrm{b} + 4\mu_\mathrm{b}}} \Big) - \frac{x_0}{\beta c B(x_0)} \Big(\frac{d_\mathrm{b} + 2\mu_\mathrm{b} + \sqrt{d_\mathrm{b}(d_\mathrm{b} + 4\mu_\mathrm{b})}}{2\sqrt{d_\mathrm{b}(d_\mathrm{b} + 4\mu_\mathrm{b})}} \Big) \right].
\end{aligned}
\tag{32}
$$

While eq. (32) gives the candidate uninvadable traits, we checked that for biologically realistic parameter values these traits are also uninvadable (e.g. for the parameter values in Fig. 3 and see SM). The corresponding (candidate) uninvadable mutation rate is given by

$$
\mu(u_\mathrm{r}^*) = \frac{(d_\mathrm{b} - \sqrt{d_\mathrm{b}}\sqrt{d_\mathrm{b} + 4\mu_\mathrm{b}})^2}{4\mu_\mathrm{b}}. \tag{33}
$$

The corresponding (candidate) uninvadable population size $N(\boldsymbol{u}^*)$ can also be explicitly expressed in terms of parameters but remains complicated (see section 2.1.4. in S.I. for the full expression). Fig. (3) illustrates the uninvadable life-history strategies $\boldsymbol{u}^* = (u_\mathrm{r}^*, u_\mathrm{m}^*)$ (panels a and b), the corresponding equilibrium population size $N(\boldsymbol{u}^*)$ (panel c), and the uninvadable mutation rate $\mu(u_\mathrm{r}^*)$ (panel d) as a function of the baseline mutation rate μ_b. This Fig. (3) demonstrates, again, that the analytically obtained results (here using eqs. 32–33) correspond very closely to those obtained by carrying out individual-based simulations of the full process (see section 2.3. in S.I. file for the Mathematica code). Overall, four main results can be drawn from Figs. (3)–Fig. (4) and eqs. (32)–(33).

First, investment into repair u_r^* at the expense of life-history functions is predicted to readily evolve and we can observe from Fig. (3a) that investment into repair u_r^* is increasing with the baseline mutation rate μ_b. However unlike in our previous example, investment into repair now also depends on the external mortality rate d_b, and $u_\mathrm{r}^* \to 1$ as external mortality vanishes $d_\mathrm{b} \to 0$ (Fig. 3b). Furthermore, in this model, investment into repair $u_\mathrm{r}^* > 0$ is always predicted to evolve.

Second, the uninvadable mutation rate $\mu(\boldsymbol{u}^*)$ monotonically increases with the baseline mutation rate μ_b. In the previous model, the uninvadable mutation rate $\mu(\boldsymbol{u}^*)$ was independent of μ_b , because the marginal benefit–to–cost ratio of repair had a simple form. In the current model however, we can observe from the selection gradient of repair (eq. 29) that both the marginal benefit of repair and the marginal cost of repair depend on the baseline mutation rate μ_b in complicated ways. The marginal benefit depends directly on μ_b, but also indirectly via its effect on the age-at-maturity v_m. The marginal cost of repair depends on the baseline mutation rate μ_b indirectly via its effect on the age-at-maturity v_m and size at maturity $x_\mathrm{m}(\boldsymbol{u}^*)$.

Third, higher levels of μ_b cause earlier age-at-maturity (smaller u_m^*, see Fig. 3b). To understand why, it is important to notice that effect of μ_b on the fitness proxy ($\tilde{R}_0(\boldsymbol{u}, \boldsymbol{v})$) is similar to the effect of the death rate d_b. This can be observed mathematically, as the marginal cost of investment into growth is given by $(\mu(v_\mathrm{r}) + d_\mathrm{b})$ (see the last term in eq. 30). Intuitively, this comes from the fact that under asexual

reproduction acquiring a mutation can be viewed similarly as death, as only members of the least-loaded class will contribute descendants far into the future (see section 2.3). Since maturing earlier causes the growth period to be shorter, the body size at maturity $x_{\mathrm{m}}(\boldsymbol{u}^*)$ will also be smaller with higher baseline mutation rate μ_{b} (Fig. 4a). Smaller body size at maturity, in turn, causes the birth rate $b_0(\boldsymbol{u}^*, \boldsymbol{u}^*)$ to be smaller (Fig. 4b). Hence, factors increasing the baseline mutation rate, cause life histories to be "faster": earlier maturation, smaller size at maturity and lower (effective) birth rates.

Fourth, higher levels of baseline mutation rate μ_{b} cause the uninvadable equilibrium population size $N(\boldsymbol{u}^*)$ to decrease and this effect is more drastic when external mortality d_{b} is higher (Fig. 3c). We can observe that the equilibrium population size $N(\boldsymbol{u}^*)$ predicted according to the classical life-history assumptions without deleterious mutations (the dashed lines in Fig. (3c); obtained at the limit $\mu(u_{\mathrm{r}}^*) \to 0$ and $u_{\mathrm{r}}^* \to 0$) is substantially higher compared to the prediction of our model. Hence, factors affecting the baseline mutation rate not only affect the evolution of life histories, but also demographic properties.

4 Discussion

Our formalisation of the long term coevolution between life-history and deleterious mutation accumulation shows that an evolutionary invasion analysis of this coevolution is tractable when the deleterious mutation rate is not too high so that the least-loaded class dominates in frequency the resident population (see section 2.3, also for relaxation of this condition). Then, the basic reproductive number of the least-loaded class (eq. 6 and eq. 9) allows to characterise the joint evolutionary stable life-history and deleterious mutation rate under a wide range of biological scenarios under asexual reproduction in age- and stage-structured populations. We analysed two specific scenarios to illustrate this invasion analysis approach: (i) coevolution between reproductive effort and the mutation rate and (ii) coevolution between the age-at-maturity and the mutation rate. These two models confirmed the validity of using the least-loaded class as a fitness proxy by comparing results to those obtained by individual-based stochastic simulations (Figs. 2–3) and provide a number of insights about life-history and deleterious mutation accumulation coevolution.

The model of the coevolution of reproductive effort with the mutation rate leads to three results. First, selection can favour physiologically costly germline repair at the expense of lowering the vital rates (survival and reproduction) (see Fig. 2a), which generalises results from population genetics (Kimura, 1967; Kondrashov, 1995; Dawson, 1998, 1999) and extends them into an explicit life-history context. Second, when allocation to repair evolves, it produces an uninvadable mutation rate ($\mu(\boldsymbol{u}^*)$) that is independent from the baseline mutation rate (Fig. 2c) and depends only on allocation efficiency parameters. This is so because the effect of baseline mutation rate on vital rates via average expected survival cancels exactly out, which is due to the fact that the loss in expected survival is counteracted by the gain in acquiring a breeding spot that depends on the survival in the population. Third, higher baseline mutation rates cause reproduction-survival trade-off to shift towards higher allocation to reproduction at the expense of survival (Fig. 2b). Higher allocation to reproduction evolves under higher baseline mutation rate μ_{b}

because the effect of the mutations rate on fitness is similar than the effect of external mortality. When individuals in the least-loaded class acquire deleterious mutations they transition into a class of individuals that will not leave descendants in the long-run (far into the future). Hence, if the mutation rate is higher, current reproduction yields higher benefits than survival, as individuals are more likely to acquire mutations. This result extends the observation of Charlesworth (1990), who concluded from a numerical model that higher levels of a fixed mutation rate (no repair) causes higher allocation to reproduction over survival. Here we extend the results of Charlesworth (1990) for a model with evolving mutation rate and, furthermore, we predict that the shift in survival-reproduction trade-off towards reproduction is stronger under: (i) the conditions of low efficiency in converting resources into vital rates (e.g. in environments with low quality nutrition), (ii) high external mortality rates (e.g. in environments with high predation rates), and (iii) high baseline mutation rates (e.g. in environments with high background radiation). We also find that immortality (complete survival) cannot evolve in our model even in an environment with no external mortality because mutation rate cannot be brought down to zero. This highlights the less appreciated role of mutation accumulation, in addition to the "extrinsic" (i.e., environmentally caused) hazards, that prevent the evolution of immortality (Medawar, 1952; Hamilton, 1966; Charlesworth, 1994). This means that forces of selection on survival and reproduction (Hamilton, 1966) decline also due to mutation rate. Overall, this example reveals that, endogenous and/or exogenous factors that increase baseline mutation rate cause higher investment into reproduction and lower investment into survival, while the observed mutation rate remains constant.

The model of the coevolution of age-at-maturity and the mutation rate leads to four results. First, as in the previous example, selection can favour highly physiologically costly germline repair at the expense of lowering the investment into life-history functions (here, into growth and reproduction, see Fig. 3a). Second, unlike in the previous example, the uninvadable mutation rate ($\mu(\boldsymbol{u}^*)$) is always predicted to increase with the baseline mutation rate (Fig. 3d). Third, the mutation rate coevolution causes earlier maturity and onset of reproduction at the expense of investing longer into growth (Fig. 3b). This results extends the observation of Dańko et al. (2012) from a numerical model that looked at the effect of fixed mutation rate on the age-at maturity. While Dańko et al. (2012) found that higher fixed mutation rate (no repair) causes earlier age-at-maturity, they concluded that this effect would be relatively small and would be observable only under extreme conditions. Here, we extend this result to a setting with evolving mutation rate and show that the effect of mutation on life-history trade-offs can be significant. Furthermore, we find that the shift in growth-reproduction trade-off towards reproduction is higher under: (i) high external mortality rates and (ii) high baseline mutation rates. Fourth, higher baseline mutation rate causes smaller equilibrium population size. While this result is well known in population genetics and has been used to study the speed of mutational meltdowns (Lynch et al., 1993; Gabriel et al., 1993), we here extended it to an explicit life-history context. Overall, we thus find that factors that increase baseline mutation rate cause higher investment into reproduction and lower investment into growth resulting in earlier age-at-maturity and smaller size at maturity, higher uninvadable mutation

rate, and lower equilibrium population size.

The analysis of these two models suggests two general findings about how life-histories co-evolve with deleterious mutation rates. First, the trade-off between lowering the rate of mutations vs investing into life-history functions affect the evolutionary outcome of life-history trade-offs (e.g. survival–vs–reproduction or growth–vs–reproduction). Hence, mutation accumulation can have a significant effect on life-history evolution through the process of coevolution that previous studies focusing on the effect of fixed mutation rates on life-history evolution have not revealed (Charlesworth, 1990; Dańko et al., 2012). Looking at the effect of fixed mutation rates on life-history evolution underestimates the effect of deleterious mutation accumulation on life-history evolution, as it does not take into account the effect of the physiological cost of immutability on life-history evolution. Second, factors that contribute to higher baseline mutation rate selects for "faster" life-histories: higher investment into current reproduction at the expense of survival and earlier age–at–maturity. Factors that could increase the baseline mutation rate μ_{b} include factors that increase DNA replications errors (number of germ-line cell divisions) or environmental mutagens (radiation level, oxygen level, nutrition quality).

We believe that our evolutionary invasion analysis approach could be usefully applied to understand several open questions in life-history theory. First, it can be directly applied to study evolution of ageing by allowing for physiological damage to accumulate over age and thus it can affect the vital rates. This would allow to develop a evolutionary model of ageing that unifies the mutation accumulation and disposable soma theories of ageing (Medawar, 1952; Kirkwood, 1977). Second, the approach can be applied to connecting the cost of germline repair with the "problem of the missing trade-offs" (e.g. Maklakov and Immler, 2016; Flatt and Partridge, 2018) and to generate more detailed predictions about the conditions under which the cost of germline repair is likely to play an important role. Third, our approach can be extended to study the Lansing effect, a widely reported negative effect of parental age to offspring fitness (e.g. Monaghan et al., 2020), for example, by providing predictions about when a stronger form of the Lansing effect would be more likely to be observed. Our analysis can also be applied to study central questions in mutation accumulation theory. For example, the classical mutation accumulation theory is not able to explain the observed variation of mutation rates in different taxa of higher eukaryotes and it has been suggested that life-history could be a missing piece in the puzzle of explaining these patterns in mutation rates (Drake et al., 1998).

In conclusion, the physiological cost of lowering the mutation rate connects life-history trade-offs and (deleterious) mutation accumulation. Studying the evolution of the interaction between life history and mutation rate can enrich the understanding of diverse array of biological phenomena from the evolution of ageing to patterns of mutation rate evolution. Our hope is that the formalisation proposed here can be fruitfully used to this end.

Appendix A: Continuous time invasion process with mutation accumulation

In section (2.2.2), we presented the renewal equation and growth rate for a discrete time process (eqs. 2–8). Let us now consider that time is continuous and that age-structure is likewise continuous so that $\mathcal{T} = [0, \infty)$. For this case, accounting entails that the expected number $n_i(t)$ of individuals at time t that descend from a single newborn (age class zero) ancestor residing at $t = 0$ in class $\mathcal{C}_i$ satisfies

$$n_i(t) = \tilde{l}_i(t) + \int_0^t n_i(t-a)\tilde{b}_i(a)\tilde{l}_i(a)\,\mathrm{d}a, \tag{A.1}$$

where all quantities maintain the same interpretation as in the discrete time case.

Eq. (A.1) is functionally equivalent to the standard renewal equation of population dynamics for continous age-structured populations (Charlesworth, 1994, eq. 1.41). As such, and as for the discrete time case, it then follows from the standard results of population dynamic processes in age-structured populations (Charlesworth, 1994, p. 27) that asymptotically, as $t \to \infty$, the number $n_i(t)$ grows geometrically as

$$n_i(t) \sim \rho_i^t K_i, \tag{A.2}$$

where K_i is some constant depending on the process and $\rho_i = \exp(r_i)$, where r_i is the mutant growth rate (or Malthusian parameter), which is the unique root of the Euler-Lotka equation

$$\int_0^\infty \exp(-ar_i)\tilde{b}_i(a)\tilde{l}_i(a)\,\mathrm{d}a = 1. \tag{A.3}$$

References

Altenberg, L. 2009. The evolutionary reduction principle for linear variation in genetic transmission. Bull. Math. Biol. 71:1264–1284.

Altenberg, L., U. Liberman, and M. W. Feldman. 2017. Unified reduction principle for the evolution of mutation, migration, and recombination. Proc. Natl. Acad. Sci. U.S.A. 114:E2392–E2400.

Avila, P., T. Priklopil, and L. Lehmann. 2021. Hamilton's rule, gradual evolution, and the optimal (feedback) control of phenotypically plastic traits. J. Theor. Biol. 526:110602.

Bürger, R. 2000. The Mathematical Theory of Selection, Recombination, and Mutation. John Wiley and Sons, New York.

Case, T. J. 2000. An Illustrated Guide to Theoretical Ecology. Oxford University Press, Oxford.

Caswell, H. 2000. Matrix Population Models. Sinauer Associates, Massachusetts.

Charlesworth, B. 1990. Optimization models, quantitative genetics, and mutation. Evolution 44:520–538.

———. 1994. Evolution in Age-Structured Populations. 2nd ed. Cambridge University Press, Cambridge.

Charnov, E. L. 1993. Life history invariants: some explorations of symmetry in evolutionary ecology. Oxford University Press, New York.

Chen, H.-y., C. Jolly, K. Bublys, D. Marcu, and S. Immler. 2020. Trade-off between somatic and germline repair in a vertebrate supports the expensive germ line hypothesis. Proc. Natl. Acad. Sci. U.S.A. 117:8973–8979.

Dańko, M. J., J. Kozlowski, J. W. Vaupel, and A. Baudisch. 2012. Mutation accumulation may be a minor force in shaping life history traits. PLoS One 7:e34146.

Dawson, K. J. 1998. Evolutionarily stable mutation rates. J. Theor. Biol. 194:143–157.

———. 1999. The dynamics of infinitesimally rare alleles, applied to the evolution of mutation rates and the expression of deleterious mutations. Theor. Popul. Biol. 55:1–22.

Day, T., and P. D. Taylor. 1996. Evolutionarily stable versus fitness maximizing life histories under frequency-dependent selections. Proc. R. Soc. B: Biol. Sci. 263:333–338.

———. 1997. Hamilton's rule meets the Hamiltonian: Kin selection on dynamic characters. Proc. R. Soc. B: Biol. Sci. 264:639–644.

———. 2000. A generalization of Pontryagin's maximum principle for dynamic evolutionary games among relatives. Theor. Popul. Biol. 57:339–356.

Drake, J. W., B. Charlesworth, D. Charlesworth, and J. F. Crow. 1998. Rates of spontaneous mutation. Genetics 148:1667–1686.

Eigen, M. 1971. Selforganization of matter and the evolution of biological macromolecules. Naturwissenschaften 58:465–523.

Eshel, I. 1983. Evolutionary and continuous stability. J. Theor. Biol. 103:99–111.

———. 1996. On the changing concept of evolutionary population stability as a reflection of a changing point of view in the quantitative theory of evolution. J. Math. Biol. 34:485–510.

Eshel, I., and M. W. Feldman. 1984. Initial increase of new mutants and some continuity properties of ess in two-locus systems. Am. Nat. 124:631–640.

Eyre-Walker, A., and P. D. Keightley. 2007. The distribution of fitness effects of new mutations. Nature Reviews Genetics 8:610–618.

Ferrière, R., and M. Gatto. 1995. Lyapunov exponents and the mathematics of invasion in oscillatory or chaotic populations. Theor. Popul. Biol. 48:126–171.

Fisher, R. A. 1930. The Genetical Theory of Natural Selection. Clarendon Press, Oxford.

Flatt, T., and L. Partridge. 2018. Horizons in the evolution of aging. BMC Biol. 16:1–13.

Frank, S. A. 2008. All of life is social. Curr. Biol. 16:R648–R650.

Gabriel, W., M. Lynch, and R. Bürger. 1993. Muller's ratchet and mutational meltdowns. Evolution 47:1744–1757.

Geritz, S. A. H., E. Kisdi, G. Meszéna, and J. A. J. Metz. 1998. Evolutionarily singular strategies and the adaptive growth and branching of the evolutionary tree. Evol. Ecol. 12:35–57.

Gillespie, J. H. 2004. Population Genetics: a Concise Guide. Johns Hopkins University Press, Baltimore, Maryland.

Haigh, J. 1978. The accumulation of deleterious genes in a population—muller's ratchet. Theor. Popul. Biol. 14:251–267.

Hamilton, W. D. 1966. The moulding of senescence by natural selection. J. Theor. Biol. 12:12–45.

Iwasa, Y., and J. Roughgarden. 1984. Shoot/root balance of plants: optimal growth of a system with many vegetative organs. Theor. Popul. Biol. 25:78–105.

Karlin, S., and H. M. Taylor. 1975. A First Course in Stochastic Processes. Academic Press, San Diego.

———. 1981. A Second Course in Stochastic Processes. Academic Press, San Diego.

Kimura, M. 1967. On the evolutionary adjustment of spontaneous mutation rates. Genet. Res. 9:23–34.

Kimura, M., and T. Maruyama. 1966. The mutational load with epistatic gene interactions in fitness. Genetics 54:1337.

Kirkwood, B. 1986. Accuracy in Molecular Processes: Its Control and Relevance to Living System. Chapman and Hall, New York.

Kirkwood, T. B. 1977. Evolution of ageing. Nature 270:301–304.

Kondrashov, A. S. 1995. Modifiers of mutation-selection balance: general approach and the evolution of mutation rates. Genet. Res. 66:53–69.

Kozlowski, J. 1992. Optimal allocation of resources to growth and reproduction: implications for age and size at maturity. Trends Ecol. Evol. 7:15–19.

Lehmann, L., C. Mullon, E. Akçay, and J. Van Cleve. 2016. Invasion fitness, inclusive fitness, and reproductive numbers in heterogeneous populations. Evolution 70:1689–1702.

Lynch, M., R. Bürger, D. Butcher, and W. Gabriel. 1993. The mutational meltdown in asexual populations. J. Hered. 84:339–344.

Maklakov, A. A., and S. Immler. 2016. The expensive germline and the evolution of ageing. Curr. Biol. 26:R577–R586.

Maynard Smith, J. 1982. Evolution and the Theory of Games. Cambridge University Press, Cambridge.

Medawar, P. B. 1952. An unsolved problem of biology. An Inaugural Lecture Delivered at University College, London.

Metz, J. A. J., S. D. Mylius, and O. Diekmann. 2008. When does evolution optimize? Evol. Ecol. Res. 10:629–654.

Metz, J. A. J., R. M. Nisbet, and S. A. H. Geritz. 1992. How should we define fitness for general ecological scenarios? Trends Ecol. Evol. 7:198–202.

Michod, R. E. 1979. Evolution of life histories in response to age-specific mortality factors. Am. Nat. 113:531–550.

Mode, C. J. 1968. A multidimensional age-dependent branching process with applications to natural selection. i. Mathematical Biosciences 3:1–18.

———. 1971. Multitype branching processes: theory and applications. 34. American Elsevier Publishing Company, New York.

Monaghan, P., A. A. Maklakov, and N. B. Metcalfe. 2020. Intergenerational transfer of ageing: parental age and offspring lifespan. Trends Ecol. Evol 35:927–937.

Monaghan, P., and N. B. Metcalfe. 2019. The deteriorating soma and the indispensable germline: gamete senescence and offspring fitness. Proc. R. Soc. B: Biol. Sci. 286:20192187.

Mullon, C., L. Keller, and L. Lehmann. 2016. Evolutionary stability of jointly evolving traits in subdivided populations. Am. Nat. 188:175–195.

Otto, S. P., and T. Day. 2007. A biologist's Guide to Mathematical Modeling in Ecology and Evolution. Princeton University Press, Princeton, NJ.

Parker, G. A., and J. Maynard Smith. 1990. Optimality theory in evolutionary biology. Science 349:27–33.

Pen, I. 2000. Reproductive effort in viscous populations. Evolution 54:293–297.

Perrin, N. 1992. Optimal resource allocation and the marginal value of organs. Am. Nat. 139:1344–1369.

Perrin, N., and R. M. Sibly. 1993. Dynamic models of energy allocation and investment. Annu. Rev. Ecol. Syst. 24.

Roff, D. A. 2008. Defining fitness in evolutionary models. J. Genet. 87:339–348.

Rousset, F. 2004. Genetic Structure and Selection in Subdivided Populations. Princeton University Press, Princeton, NJ.

Schaffer, W. M. 1982. The application of optimal control theory to the general life history problem. American Naturalist 121:418–431.

Sniegowski, P. D., P. J. Gerrish, T. Johnson, and A. Shaver. 2000. The evolution of mutation rates: separating causes from consequences. Bioessays 22:1057–1066.

Stearns, S. 1992. The Evolution of Life Histories. Oxford University Press, Oxford.

Steinsaltz, D., S. N. Evans, and K. W. Wachter. 2005. A generalized model of mutation–selection balance with applications to aging. Adv. Appl. Math. 35:16–33.

Szathmary, E., and J. Maynard Smith. 1997. From replicators to reproducers: the first major transitions leading to life. J. Theor. Biol. 187:555–571.

Taylor, P. D. 1989. Evolutionary stability in one-parameter models under weak selection. Theor. Popul. Biol. 36:125–143.

Van Cleve, J. 2015. Social evolution and genetic interactions in the short and long term. Theor. Popul. Biol. 103:2–26.

Van Cleve, J., and L. Lehmann. 2013. Stochastic stability and the evolution of coordination in spatially structured populations. Theor. Popul. Biol. 89:75–87.

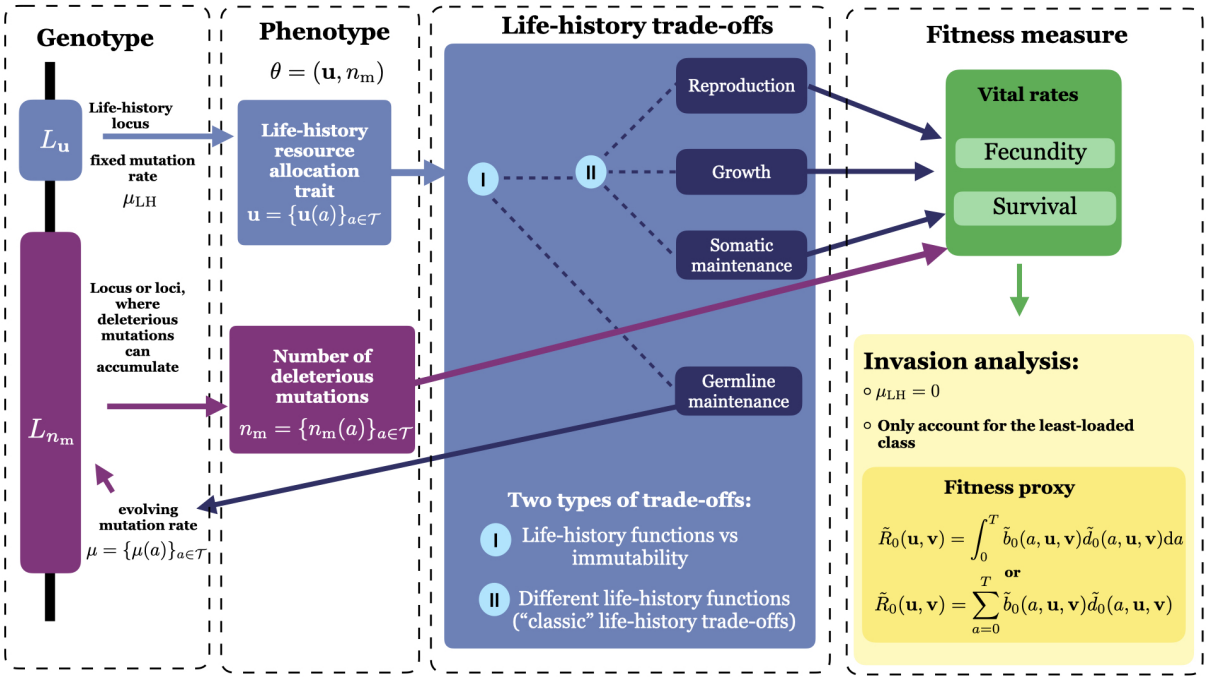

Figure 1: Key components of the life-history model with mutation accumulation. An individual's genotype is characterised by a life-history locus $L_{\boldsymbol{u}}$ and a deleterious mutation locus/loci (purple rectangle) L_{n_m}. The mutation rate at the life-history locus μ_{LH} is considered to be fixed, while the mutation rate μ at the deleterious mutation locus depends on the life-history trait $\boldsymbol{u}$ and is evolving. The phenotype of an individual $\theta = (\boldsymbol{u}, n_\mathrm{m})$ is given by the life-history allocation trajectory $\boldsymbol{u} = \{\boldsymbol{u}(a)\}_{a\in\mathcal{T}}$ and the number of deleterious mutations accumulated $n_\mathrm{m} = \{n_\mathrm{m}(a)\}_{a\in\mathcal{T}}$ throughout lifespan. The resource allocation trait captures two different types of trade-offs: (i) between immutability vs life-history and (ii) between different life-history functions themselves ("classic" life history trade-offs, e.g. Stearns, 1992; Roff, 2008). Hence, the life-history locus affects the vital rates and thus fitness directly through different life-history functions and indirectly through allocation to immutability since vital rates depend on the number of deleterious mutations. For the invasion analysis we assume $\mu_{LH} = 0$, thus only considering a mutant-resident system and use the basic reproductive number of the least-loaded class $\tilde{R}_0$ as a fitness proxy (as detailed in section 2.3). For carrying out individual-based stochastic simulations (see section 3 and sections 1.3 and 2.3 in the S.I.), we let $\mu_{LH} > 0$ but keep it small, which makes the full coevolutionary process irreducible (see also discussion section 2.3).

(a) Uninvadable investment into repair u_r^*.

(b) Uninvadable investment into survival u_s^*.

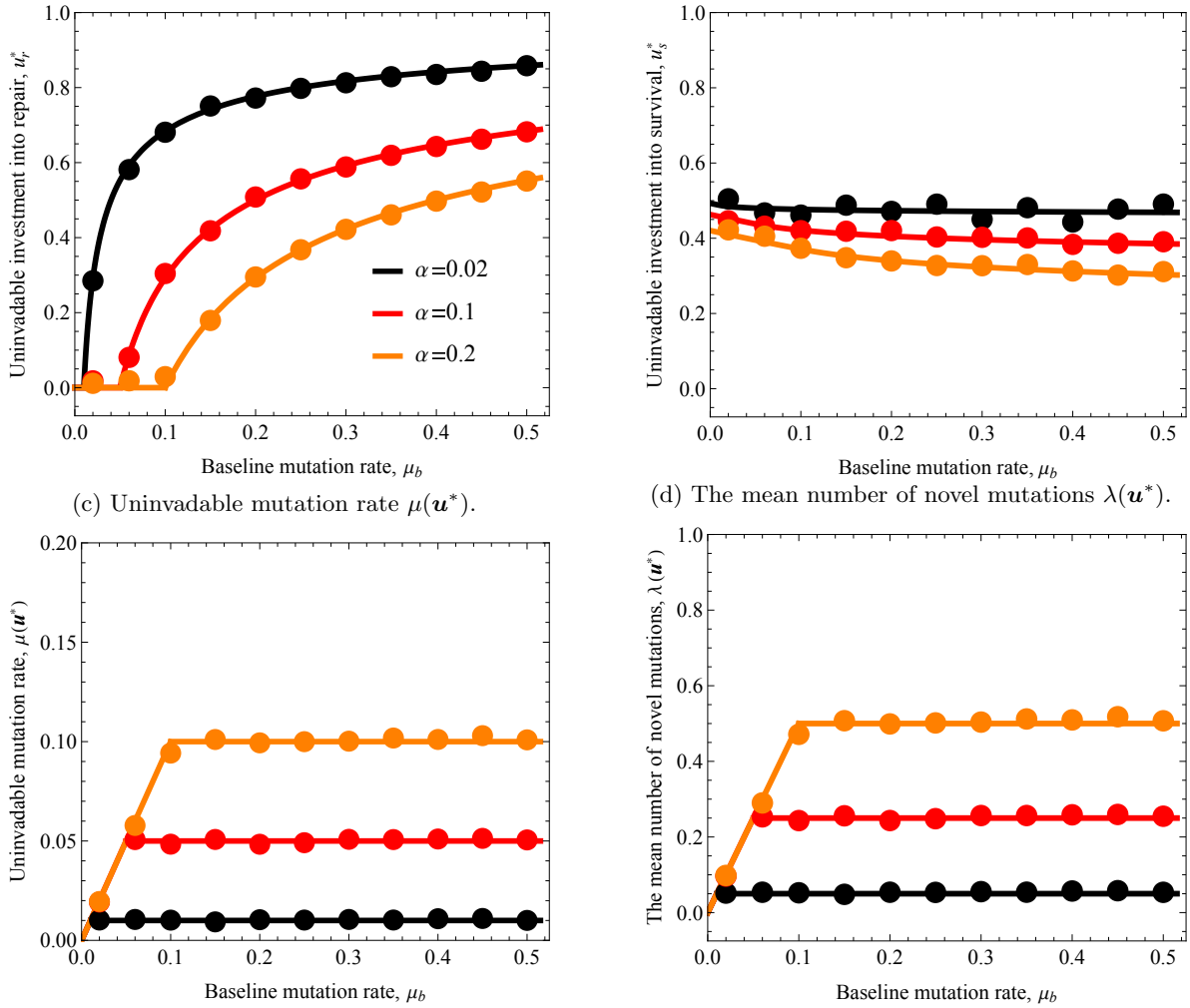

(c) Uninvadable mutation rate $\mu(\boldsymbol{u}^*)$.

(d) The mean number of novel mutations $\lambda(\boldsymbol{u}^*)$.

Figure 2: Predictions from the analytical model (solid lines) and from individual-based simulations of a finite population (circles) for the uninvadable life-history strategies $\boldsymbol{u}^* = (u_r^*, u_s^*)$ (panel a and b) and the mean number of novel mutations $\lambda(\boldsymbol{u}^*)$ (panel c) as functions of baseline mutation rate μ_b. The solution for the individual-based simulations are obtained as time-averages measured over 7500 generations while starting the simulation at the analytically predicted equilibrium (see S.I. section 1.3 for details about the simulation code and we note that convergence towards the equilibria was checked to occur in simulations). The different colours represent different values of efficiency of fecundity and survival parameter α. Parameter values: $f_b = 5$, $\alpha_\mu = 2$, $s_b = 0.5$, $\sigma = \sigma_f = \sigma_s = 0.2$; for simulations: $N = 7500$, $f_b = 0$, $s_b = 0.5$.

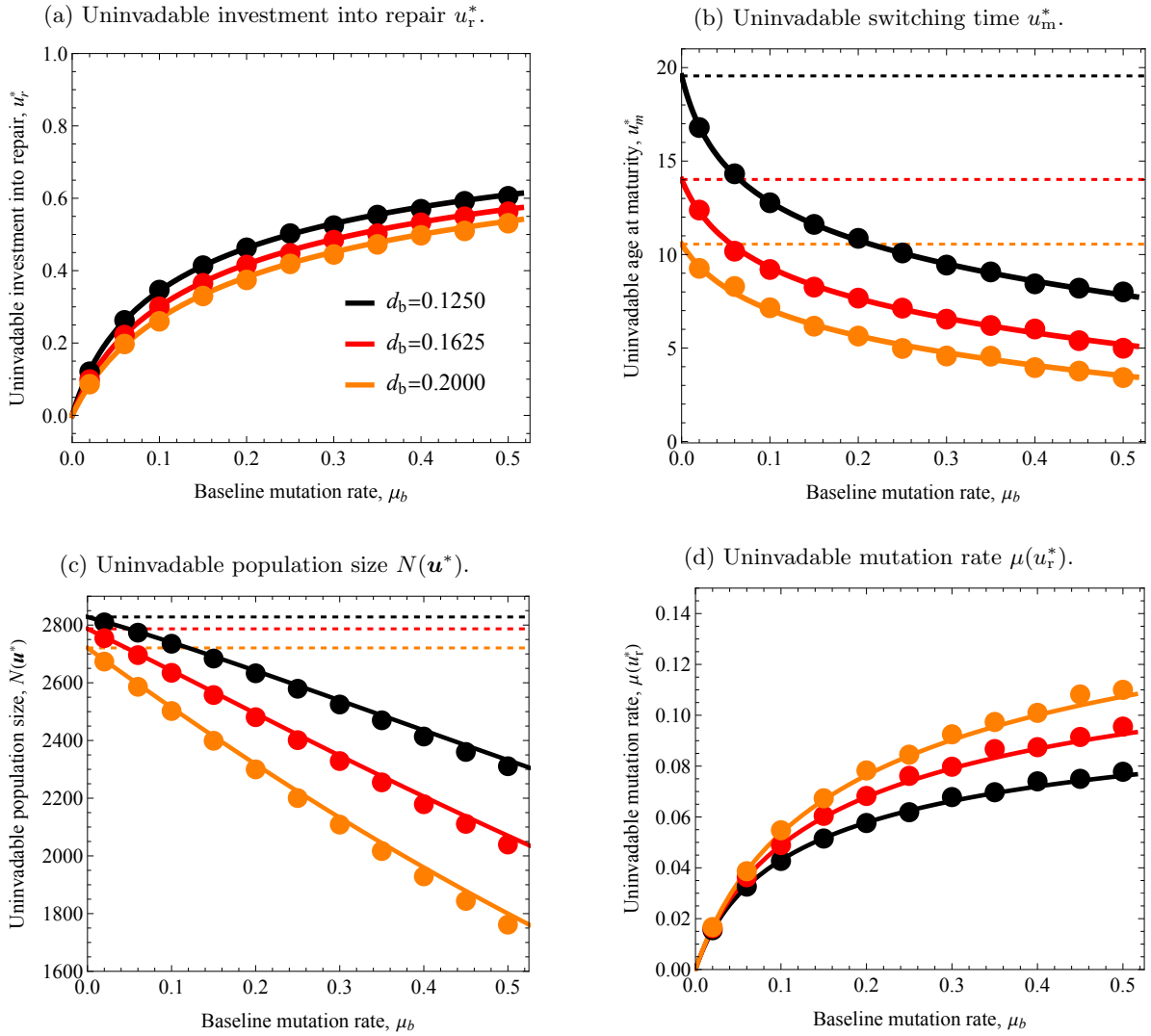

Figure 3: Predictions from the analytical model (solid lines) and from individual-based simulations (circles obtained as averages) for uninvadable life-history strategies $\boldsymbol{u}^* = (u_m^*, u_r^*)$ (panel a and b), population size $N(\boldsymbol{u}^*)$ (panel c) and mutation rate $\mu(u_r^*)$ as functions of baseline mutation rate μ_b for different values of baseline mortality d_b ($d_b = 0.1250$ - black, $d_b = 0.1625$ - red, $d_b = 0.2$ - orange). The dashed lines represent the "classical life-history" prediction (i.e. when $\mu(u_r^*) \to 0$ and $u_r^* \to 0$), where the colours of the dashed represent the different values for d_b parameter and match the values of solid lines ($d_b = 0.1250$ - black, $d_b = 0.1625$ - red, $d_b = 0.2$ - orange). The solution for the individual-based simulations are obtained as time-averages measured over 3000 "generations" while starting the simulation at analytically predicted equilibrium for the trait values and population size (see S.I. section 2.3 for the code and for more details). The different colours represent different values of baseline mortality rate d_b. Parameter values: $\sigma = \sigma_b = \sigma_d = 0.2$, $x_0 = 1$, $a = 0.9$, $c = 0.75$, $\gamma = 0.00035$, $\beta = 1$, $\mu_f = 0$.

(a) Uninvadable body size at maturity $x_{\mathrm{m}}(\boldsymbol{u}^*)$.

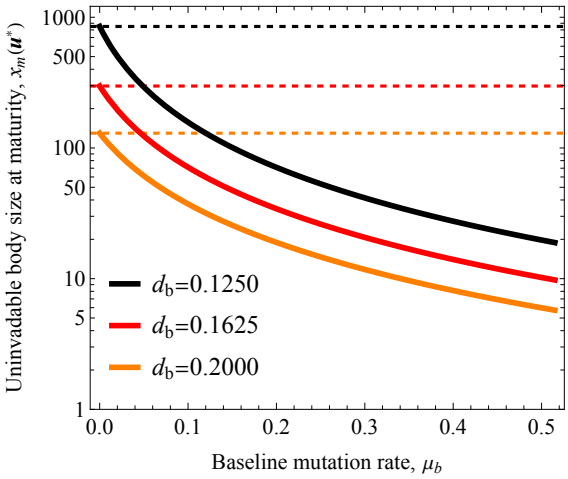

(b) Uninvadable (effective) birth rate $b_0(\boldsymbol{u}^*, \boldsymbol{u}^*)$.

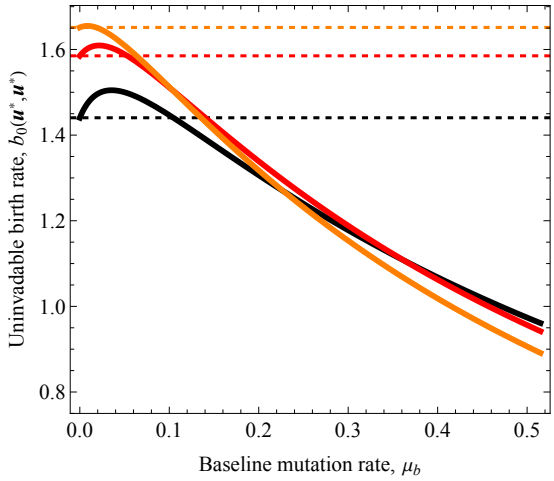

Figure 4: Predictions from the analytical model for the uninvadable body size at maturity $x_{\mathrm{m}}(\boldsymbol{u}^*)$ and the (effective) birth rate $b_0(\boldsymbol{u}^*, \boldsymbol{u}^*)$ as a function of baseline mutation rate for different values of mortality rate d_{b} ($d_{\mathrm{b}} = 0.1250$ - black, $d_{\mathrm{b}} = 0.1625$ - red, $d_{\mathrm{b}} = 0.2$ - black). The dashed lines represent the "classical life-history" prediction (i.e. when $\mu(u_{\mathrm{r}}^*) \to 0$ and $u_{\mathrm{r}}^* \to 0$), where the colours of the dashed represent the different values for d_{b} parameter and match the values of solid lines ($d_{\mathrm{b}} = 0.1250$ - black, $d_{\mathrm{b}} = 0.1625$ - red, $d_{\mathrm{b}} = 0.2$ - black). Parameter values: $\sigma = \sigma_{\mathrm{b}} = \sigma_{\mathrm{d}} = 0.2$, $x_0 = 1$, $a = 0.9$, $c = 0.75$, $\gamma = 0.00035$, $\beta = 1$, $\mu_{\mathrm{f}} = 0$.